Modeling and Control of Bidirectional DC DC Converter Fed PMDC Motor

(for HEV Applications)

Thesis submitted in partial fulfillment of the requirements for the degree of

Master of Technology

in

Electrical Engineering

(Specialization: Control & Automation)

by

Mahendra Chandra Joshi

Department of Electrical Engineering
National Institute of Technology Rourkela
Rourkela, Odisha, 769008, India

May 2013

Modeling and Control of Bidirectional DC DC Converter Fed PMDC Motor

(for HEV Applications)

Dissertation submitted in

in May 2013

to the department of

Electrical Engineering

of

National Institute of Technology Rourkela

in partial fulfillment of the requirements for the degree of

Master of Technology

by

Mahendra Chandra Joshi

(Roll 211EE3336)

under the supervision of

Prof. Susovon Samanta

Department of Electrical Engineering
National Institute of Technology Rourkela
Rourkela, Odisha, 769008, India

Department of Electrical Engineering
National Institute of Technology Rourkela
Rourkela-769008, Odisha, India.

Certificate

This is to certify that the work in the thesis entitled ***Modeling and Control of Bidirectional DC DC Converter Fed PMDC Motor (for HEV Applications)*** by ***Mahendra Chandra Joshi*** is a record of an original research work carried out by him under my supervision and guidance in partial fulfillment of the requirements for the award of the degree of Master of Technology with the specialization of **Control** & **Automation** in the department of **Electrical Engineering**, National Institute of Technology Rourkela. Neither this thesis nor any part of it has been submitted for any degree or academic award elsewhere.

Place: NIT Rourkela
Date: May 2013

Prof. Susovon Samanta
Professor, EE Department
NIT Rourkela, Odisha

Acknowledgment

First and Foremost, I would like to express my sincere gratitude towards my supervisior Prof. Susovon Samanta for his advice during my project work. He has constantly encouraged me to remain focused on achieving my goal. His observations and comments helped me to establish the overall direction of the research and to move forward with investigation in depth. He has helped me greatly and been a source of knowledge.

I extend my thanks to our HOD, Prof. A.K Panda and to all the professors of the department for their support and encouragement.

I am really thankful to my batchmates especially Raghu, Usha, Vimal, and Ankush who helped me during my course work and also in writing the thesis . Also I would like to thanks my all friends particularly Amit, Narendra, Piyush and Tanmay for their personal and moral support. My sincere thanks to everyone who has provided me with kind words, a welcome ear, new ideas, useful criticism, or their invaluable time, I am truly indebted.

I must acknowledge the academic resources that I have got from NIT Rourkela. I would like to thank administrative and technical staff members of the Department who have been kind enough to advise and help in their respective roles.

Last, but not the least, I would like to acknowledge the love, support and motivation I recieved from my parents and therefore I dedicate this thesis to my family.

Mahendra Chandra Joshi
211EE3336

Abstract

The present work aims at designing and modelling of a bidirectional DC DC converter for driving a Permanent Magnet DC (PMDC) motor for Hybrid Electric Vehicle (HEV) and Electric Bikes (EV) application. Permanent Magnet Brushed DC (PMBDC) motors and Permanent Magnet Brushless DC (PMBLDC) motors are the most popular options that are used for the integration of an electric bicycle and bikes. But despite of the simple controllers and low cost of the PMDC motor its lower efficiency sets it back in choice in the present scenario as compared to the BLDC motors. The present design aims at improving the efficiency of the PMDC motor traction drive system by the incorporation of the bidirectional DC DC converter between the electrical source and the traction motor which in addition to its primary function of providing the traction energy, also facilitates the energy regeneration during braking (in the case of HEV and EV) and during the motion along down the slope(in case of a pedalled electric bicycle).The incorporation of the regenerative braking can improve the efficiency of the traction drive as much as 25% and therefore improve the driving range. During motoring operation the converter operates in the step up mode (boost mode) to provide the energy from the battery to the traction motor while during regeneration the motor acts as a generator and the DC DC converter operates in step down mode(buck mode) to recharge the battery. Half Bridge non-isolated bidirectional DC DC converter topology has been selected for the present work of study because of the absence of the transformer which reduces the weight of the system and therefore the size and the cost of the system considerably reduces. Non isolated half bridge topology is the appropriate option for the systems requiring high power applications as well as systems having constraints on their size and weight or both such as spacecraft applications, HEVs and the electric bicycle. Furthermore the switching losses in conventional converters can be reduced by using soft switching techniques. Zero Voltage Resonant Soft Switching (ZVRT) technique has been used for the power conversion in the present work to reduce the power devices switching losses. ZVRT

switching has been achieved by the use of complimentary gate switching method. Also the use of the ZVRT techniques requires the discontinuous Conduction Mode (DCM) of the inductor, which further reduces the inductor size. Although the use of the DCM increases the ripples, the same can be reduced by the interleaving technique. Also the parasitic ringing of the voltage across the mosfets whenever the current reaches zero due to the parasitic capacitances of the devices have been eliminated with the ZVRT soft switching. The power stage modelling of the converter fed pmdc motor model has been proposed and the state space averaged equations have been designed for the same. Conventionally the bidirectional DC DC converters are designed with the voltage source on both the sides, but the present work proposes the converter power stage directly feeding the PMDC motor. Hence the additional motor parameters affect the design, selection and optimization of the various converter parameters values. Thus the power stage consisting of the voltage source(battery) on one side and the PMDC motor on the other side turns out to be a fifth order system with five energy elements viz an inductor and two capacitors of the converter as well as the armature inductor and the moment of inertia of the motor. With the PMDC motor directly fed by the converters power stage, the whole systems modelling turns out to be an electromechanical system with multiple variables, and since there is not a wider possibility of selecting the component values of the various parameters of a PMDC motor with a specified rating available in the market, all that turns out to fulfil the design requirements is to judiciously compromise with the converters parameters to meet the various specifications of the system. The state space averaged model has been used to determine the various input-output transfer functions of the system. In the present work, the speed and the regenerative braking of the PMDC motor has been controlled by the duty cycle of the switches .A unified controller has been designed and simulated for the control of the both the modes i.e. motoring as well as regeneration.

Contents

List of Figures

List of Abbreviations

BLDC	:	Brushless Direct Current
CCM	:	Continuous Conduction Mode
D	:	duty ratio
DC	:	Direct Current
DCM	:	Discontinuous Conduction Mode
EMI	:	Electromagnetic Interference
HEV	:	Hybrid Electric Vehicle
Hz	:	Hertz
IC	:	Integrated Circuit
ICE	:	Internal Combustion Engine
IGBT	:	Insulated Gate Bipolar Transistor
MOSFET	:	Metal Oxide Semiconductor Field Effect Transistor
PMBLDC	:	Permanent Magnet Brushless Direct Current
PMDC	:	Permanent Magnet Direct Current
PV	:	Photovoltaic
SOC	:	State of Charge
ZCS	:	Zero Current Switching
ZVS	:	Zero Voltage Switching
ZVRT	:	Zero Voltage Resonance Transition

Chapter 1

Introduction

Chapter 1

Introduction

1.1 Background

Petroleum resources across the world is depleting at a high rate due to the large dependency of the transportation sector on petroleum as the primary fuel. Also due to this, there is a vast greenhouse gas emission that is degrading the quality of air and causing harm to life and environment. This has aroused a tremendous interest for the design of the vehicles with lesser or no dependency on the petroleum resources. And therefore the alternate propulsion technologies have been increasingly pursued by the automobile industries and this has led to the increased development rate of the of the Hybrid Electric Vehicle (HEV) technology in the past two decades. The first HEV car was introduced during 1900 by Lohner Coach Factory, which was driven by a hub motor powered by the generator run through a gasoline engine with a small battery for reliability. But since then due to the better development in the ICE technologies and the cheaper petroleum prices made the ICE run vehicle a better option than a HEV. Therefore the growth of the HEV technologies remained almost stagnant until recent past two decades when the petroleum prices started rising due to their limited availability and greater consumption as well as because of the degrading atmospheric and environmental conditions because of the emissions due to hydrocarbon combustion . An HEV unlike conventional vehicle, which depends solely on the ICE engine for the traction power, utilizes electrical energy storage in combination with the ICE to provide the required traction power. Thus it facilitates the improvement in the energy

conversion of the vehicle thereby increasing the efficiency and drivability and at the same time reducing the emissions. Furthermore the integration of the electrical storage system also makes the provision for the regeneration during braking which can further boost up the efficiency of the overall system.

1.2 Motivation

One of the main considerations for the HEV drive train is to improve the efficiency of the motor drive. This can be done by increasing the voltage level of the ESS and thereby reducing the high currents and thus the associated losses. The increase in the voltage level of the ESS can be done by the addition of the more number of the cells in the battery back of the ESS of the HEV. Although it increases the voltage level but at the same time it also increases the weight, size and cost of the system which is obviously not a desirable option for a vehicular application which has constraints on its size and weight. The other option is to use a bidirectional DC DC converter. Bidirectional DC DC converters boost up the voltage level of the electrical storage system to the higher voltage level and thereby reducing the current level and hence the losses. Also Bidirectional DC DC converter facilitates the provision for the reverse power flow back into the ESS during regenerative braking and hence further increasing the efficiency. This two features of the Bidirectional DC DC converter makes it a better option for power conversion in the HEV drivetrain thereby reducing overall cost ,size and weight of the system along with increasing efficiency and achieving regenerative energy .

1.3 Contribution of the Thesis

The primary objective of this work is to design, model and simulate the Bidirectional DC DC converter fed PMDC motor. In accordance with this objective, the methodology for selecting an appropriate topology of the bidirectional DC DC converter has been presented and then the power stage of the converter directly feeding the PMDC motor has been designed to meet the required specifications. Some of the salient points of this thesis are:

1. Development of converter fed PMDC motor Power Stage Model .
2. Unified Controller during both the modes for the speed control of the PMDC motor.
3. Controlled regeneration during Braking and downhill motion to charge the battery.
4. Incorporation of Soft Switching technique to reduce the switching losses in the motor fed converter.
5. Reduced electromagnetic interference(EMI) due to the elimination of parasitic ringing in the converter
6. Converter circuit parameter design procedure.

1.4 Literature Review

With the purpose of improving the efficiency of the drivetrain and to minimize the dependency on the petroleum fuels two or more sources of the propulsions (including ICE) are being employed in the vehicles . This are known as the Hybrid Electric Vehicles(HEVs). The topological overview of the various hybrid drive trains and the comparision between them has been presented in [1, 2, 4]. The role and the requirement of the power electronics and dc dc converter in the HEV technology was reviewed and explained in [3, 5]. The comparision between the various non isolated Bidirectional DC DC converters on the basis of their performance has been done in [7,8,13]. Motor selection and the various drive train issues depending up on the traction drive requirements and operational performance has been done in [15, 16]. The power stage design methodology and the ZVRT switching was introduced in [19]. It also the implemented the DCM operation for the power density maximization of the converter. The concepts of the soft switching techniques for the efficiency improvement and the device stress reduction was presented in the [24, 25]. The unified controller for a current mode controlled bidirectional DC DC converter was presented in [26, 28].

1.5 Organization of the Thesis

The thesis work has been organized as follows:

- **Chapter 2:** provides an overview of the various bidirectional DC DC converter topologies and the various motors used for the HEV and electric bikes application.
- **Chapter 3:**deals with the circuit operation and the design issues. First the circuit specification has been provided and consequently the design objectives have been set to fulfill the satisfactory operation of the converter.
- **Chapter 4:** in this chapter, modeling and controller design has been described for the converter circuit.
- **Chapter 5:** presents the simulation results and the analysis along with future work and conclusion.

Chapter 2

Bidirectional DC DC Converter Topology and Motor Selection

Chapter 2

Bidirectional DC DC Converter Topology and Motor Selection

2.1 Bidirectional DC DC Converters

Bidirectional DC DC converters serves the purpose of stepping up or stepping down the voltage level between its input and output along with the capability of power flow in both the directions. Bidirectional DC DC converters have attracted a great deal of applications in the area of the energy storage systems for Hybrid Vehicles , Renewable energy storage systems, Uninterruptable power supplies and Fuel cell storage systems. Traditionally they were used for the motor drives for the speed control and regenerative braking. Bidirectional DC DC converters are employed when the DC bus voltage regulation has to be achieved along with the power flow capability in both the direction. One such example is the power generation by wind or solar power systems, where there is a large fluctuation in the generated power because of the the large variation and uncertainty of the energy supply to the conversion unit (wind turbines & PV panels) by the primary source. These systems cannot serve as a standalone system for power supply because of these large fluctuations and therefore these systems are always backed up and supported by the auxiliary sources which are rechargeable such as battery units or super capacitors. This sources supplement the main system at the time of energy deficit to provide the power at regulated level and gets recharged through main system at the time of surplus power generation or at their lower threshold level of discharge. Therefore a bidirectional DC DC converter is needed to be able to

allow power flow in both the directions at the regulated level.

Likewise in HEVs, bidirectional DC DC converters are employed to link up the high voltage DC bus to the hybrid electrical storage system (usually a combination of the battery or a fuel cell with the super capacitor). Here they are needed to regulate the power supply to the motor drive to assist the ICE according to the traction power demanded. The need for a bidirectional DC DC converter in the

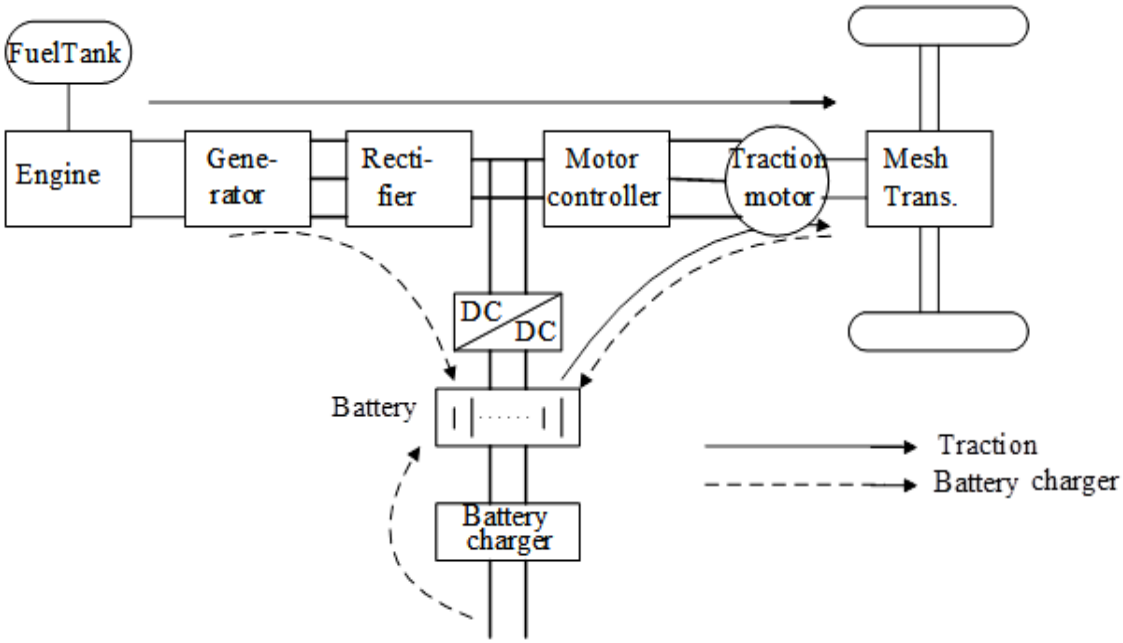

Figure 2.1: Series hybrid Drive Train employing a bidirectional DC DC converter

HEV is due to the following reasons:

1. The system is operating at the high power and low voltage making the current to rise too high, which causes high electrical and thermal stresses in the passive as well as the active components of the system, also it increases the ohmic losses and hence decrease efficiency.

2. Device voltage and current stresses is even further increased up by the wide variation in the input voltage range of the system. Since device stresses depends on the output to input voltage ratio, input voltage variation further increases the components ratings to be used.

3. Further along with the above two factors, the parasitic ringing due to the parasitic components causes EMI emission and therefore ,the proper shielding has to be provided. All above three factors makes the converter packaging bulky, heavy and expensive. Thus there is a need for an efficient DC DC converter to deal with this issue.

4. To be able to recharge the electrical energy storage system during the regenerative braking, and hence therefore there should be the provision of bidirectional power flow.

Some of the requirements for the Bidirectional DC DC converters design for the HEV applications are as follows :

- High efficiency
- Light weight & compact size
- Lower electromagnetic Interference
- Lower input and output current ripple
- Controlled power flow in spite of wide input voltage variation

Classification of Bidirectional DC DC converter

Basically, bidirectional DC DC converters can be classified into two categories depending on the Galvanic isolation between the input and output side[6]:

1. Non-Isolated Bidirectional DC DC converters
2. Isolated Bidirectional DC DC converters

2.1.1 Non-Isolated Bidirectional DC DC converters

Basically a non-isolated bidirectional DC DC converter can be derived from the unidirectional DC DC converters by enhancing the unidirectional conduction capability of the conventional converters by the bidirectional conducting switches. Due to the presence of the diode in the basic buck and boost converter circuits, they do not have the inherent property of the bidirectional power flow. This limitation in the conventional Boost and Buck converter circuits can be removed by introducing a Power Mosfet or an IGBT having an antiparallel diode across them to form a bidirectional switch and hence allowing current conduction in both directions for bidirectional power flow in accordance with the controlled switching operation.

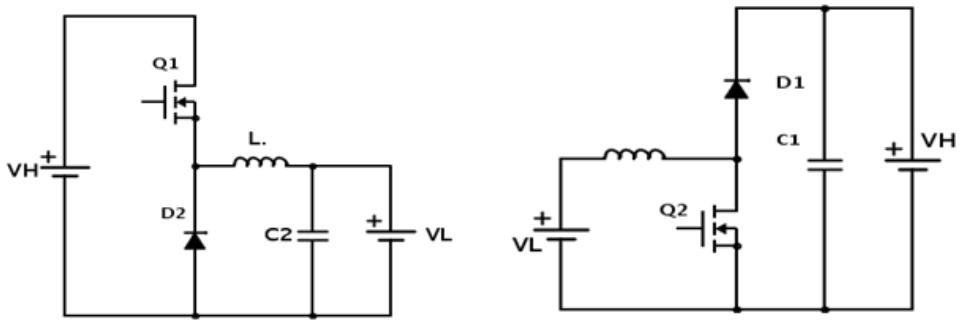

(a) (b)

Figure 2.2: (a)Buck Converter and (b)Boost Converter

Buck Boost Converter

The first bidirectional topology [7] can be directly derived from the conventional buck boost topology by the introduction of the bidirectional conducting switch as discussed above. During step up operation Switch Q1 is conducted at the required duty cycle whereas the switch Q2 is kept off all the time. Similarly during the step down operation the switch Q2 is made to conduct at required duty cycle whereas the switch Q1 is always off. Small Dead time is provided during mode transition in order to avoid the cross conductance through two switches and the converter output capacitance.

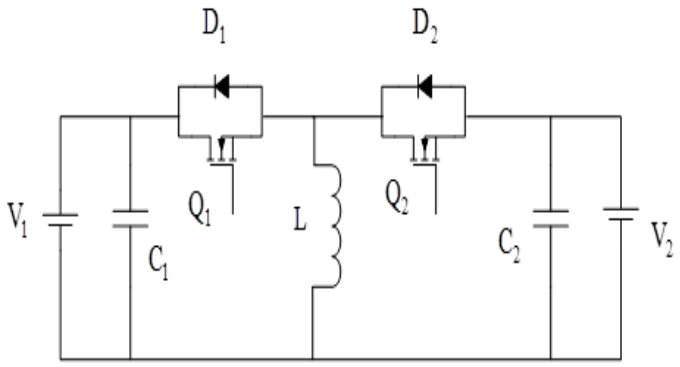

Figure 2.3: Bidirectional Buck Boost Converters

Buck Boost Cascade Converter

The second Bidirectional topology [7] as seen in the fig: 2.4 can be obtained by cascading the bidirectional buck converter with bidirectional boost converter. This topology allows the output voltage to be either higher or lower than the input voltage depending up on the switch combinations used and the direction of the current. For the step up operation in the forward direction, the switch S1 is always on and S2 and S4 are always off, whereas the switch S2 is conducted depending on the duty cycle. During forward step down operation the switch S1 is operated with the required duty cycle and the switch S2, S3, S4 are always off. Diode D2 and D3 are always reverse biased whereas the D3 is always forward biased. Diode D4 acts as a freewheeling diode. Similarly in the backward step up operation, switch S3 is always on whereas the switch S4 is operated with the required duty cycle with the diode D1 acting as a freewheeling diode.

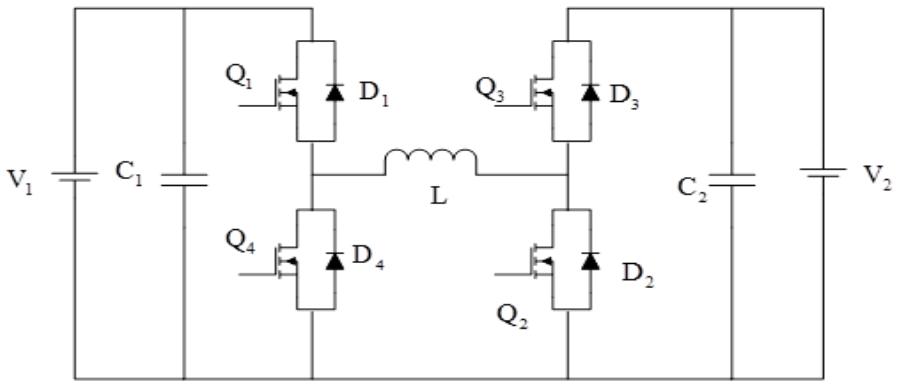

Figure 2.4: Bidirectional Cascade Buck-Boost Converter

Cuk Converter

The third topology [13] is obtained by replacing the unidirectional switches of the conventional Cuk converter by the bidirectional switches. The resulting circuit is as shown in the fig 5. The capacitor C acts as the main storage element whereas the capacitors C1 and C2 act as the coupling capacitors. It can step up or step down the input voltage like a buck-boost converter but with inverted polarity.

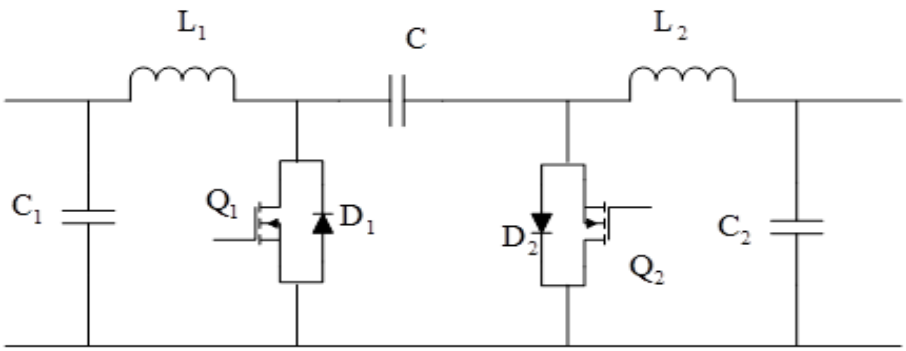

Figure 2.5: Bidirectional Cuk Converter

Half-Bridge DC DC converter

When the Buck and the boost converters are connected in antiparallel across each other with the resulting circuit is basically having the same structure as the fundamental Boost and Buck structure but with the added feature of bidirectional power flow [8,13]. The below figure shows the basic structure of the Non-Isolated Half-Bridge Bidirectional DC DC converter.

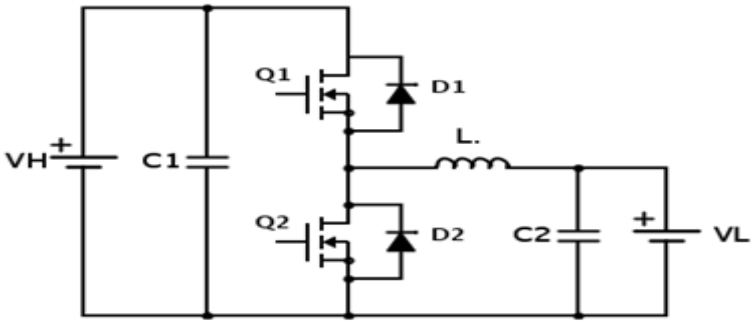

Figure 2.6: Non Isolated Half-Bridge Bidirectional DC DC Converter resulting out of the antiparallel connection of the Buck and Boost converters

The above circuit can be made to work in buck or boost mode depending on the switching of the Mosfets Q1 and Q2. The switches Q1 or Q2 in combination with the anti-parallel diodes D1 or D2 (acting as freewheeling diode) respectively, makes the circuit step up or step down the voltage applied across them. The bidirectional operation of the above circuit can be explained in the below two modes as follows:

Mode 1 (Boost Mode): In this mode switch Q2 and diode D1 enters into conduction depending on the duty cycle whereas the switch Q1 and diode D2 are off all the time. This mode can further be divided into two interval depending on the conduction on the switch Q1 and diode D2 as shown in the Fig and Fig.

Interval 1 (Q2-on, D2-off ; Q1-off, D2-Off): In this mode Q2 is on and hence can be considered to be short circuited, therefore the lower voltage battery charges the inductor and the inductor current goes on increasing till not the gate pulse is removed from the Q2 . Also since the diode D1 is reversed biased in this mode and the switch Q1 is off, no current flows through the switch Q1.

Interval 2 (Q1-off, D1-off; Q2-off, D2-on): In this mode Q2 and Q1 both are off and hence can be considered to be opened circuited. Now since the current flowing through the inductor cannot change instantaneously, the polarity of the voltage across it reverses and hence it starts acting in series with the input voltage. Therefore the diode D1 is forward biased and hence the inductor current charges the output capacitor C2 to a higher voltage. Therefore the output voltage boosts up.

Mode 2 (Buck Mode): In this mode switch Q1 and diode D2 enters into conduction depending on the duty cycle whereas the switch Q2 and diode D1 are off all the time. This mode can further be divided into two interval depending on the conduction on the switch Q2 and diode D1 as shown in the Fig and Fig.

Interval 1 (Q2-on, D2-off; Q1-off, D2-Off): In this mode Q1 is on and Q2 is off and hence the equivalent circuit is as shown in the Fig below. The higher voltage battery will charge the inductor and the output capacitor will get charged by it.

Interval 2 (Q1-off, D1-off; Q2-off, D2-on): In this mode Q2 and Q1 both are off. Again since the inductor current cannot change instantaneously, it gets discharged through the freewheeling diode D2. The voltage across the load is stepped down as compared to the input voltage.

A comparison between the different features of the non-isolated bidirectional topologies have been presented below:

1. During step up mode, in the buck-boost bidirectional converter the rms value of the current through the inductor and the power switches is greater by an amount equal to the output current as compared to the buck-boost cascade bidirectional converter. Also the capacitor rms current also exceeds in the former case by an amount of the 1/3rd of the output current. Therefore in the bidirectional buck-boost converter the inductor, power switches and the capacitor operate under more thermal and electrical stresses as compared to the buck boost cascade converter resulting in the greater power loss and also causing the saturation of the inductor core. Also since the stress on the mosfet and the diode is higher, buck-boost bidirectional converter requires power devices with larger device ratings. Higher rms currents also results in higher conduction losses and thus decreasing the overall efficiency of the buck-boost bidirectional converter .

2. However the number of devices required by the cascade buck boost converter is twice the number devices in buck-boost bidirectional converter. This problem can be solved by using the Half-Bridge Bidirectional DC DC Converter. It has the same no devices as the buck-boost bidirectional converter and can

be employed instead of the buck-boost cascade bidirectional converter for the applications that require the boost operation only in one direction and the buck in the other.

3. The main advantages of the half bridge bidirectional converter as compared to the bidirectional Cuk converter is that it only requires one inductor instead of two and that too half the value of latter as well as the power switches ratings required for the half bridge bidirectional converter is much lower as compared to the Cuk converter. Also the efficiency of the half bridge converter is higher than the Cuk converter because of the lower inductor current and therefore lower conduction as well as lower switching losses.

2.2 Isolated Bidirectional DC DC Converter

These converters can regulate a wide range of power from few watts to hundreds of kilowatts. Galvanic isolation is required in certain applications demanding Personnel safety, noise reduction as well as proper operation of protection systems. Also certain systems require voltage matching between the different stages for the proper design and the optimization of different stages. Generally Voltage matching and Galvanic isolation is achieved by the transformer in a power electronic circuitry. This necessitates the requirement of the ac link for the energy transfer. Thus the system complexity grows up with the incorporation of all this features. Basically most of the isolated bidirectional DC DC converters have the structure as shown in the fig:2.7.

This system requires two switching dc to ac converters operating at a high frequency so as to convert the dc input to high frequency ac quantities. Galvanic isolation between the source and load side is provided by the high-frequency transformer. Transformer also performs voltage matching between the source and the load side since the voltage ratio between them is very high. The transformer works with ac quantities and hence a dc-ac converter is required at both the terminals. Since the system is meant for the energy transfer in both the directions, dc to ac

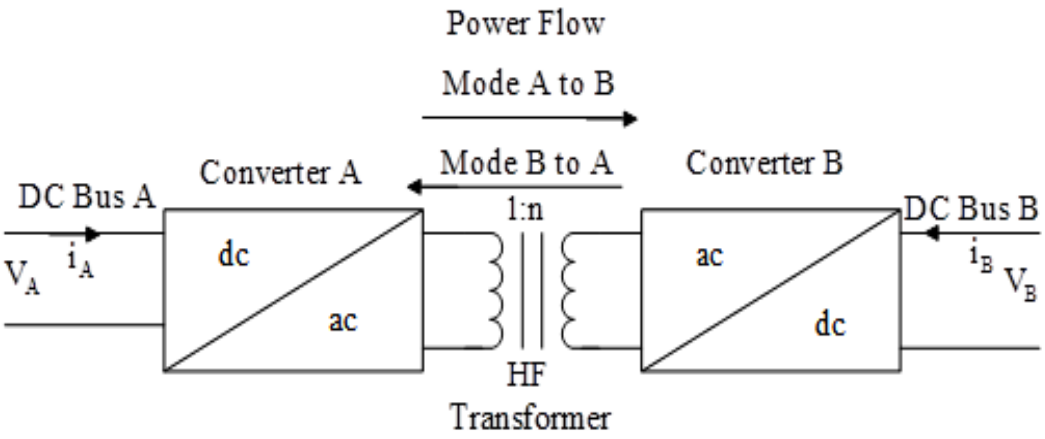

Figure 2.7: Basic Structure of an Isolated Bidirectional DC DC Converter

converters employed must have the capability of bidirectional power flow. This converters also like the non-isolated bidirectional DC DC converters works in two modes of operation i.e. in buck or boost.

Isolated bidirectional DC DC converters can be broadly classified into two categories on the basis of their configuration:

- A current fed isolated bidirectional DC DC converter has an inductor at its terminals which acts like a current source like a conventional boost converter with an inductor at the input terminals.
- A voltage fed isolated bidirectional DC DC converter as shown in the fig.2.8 has a capacitor at its terminals which acts like a voltage source like a conventional buck converter with a capacitor at its input terminals.

Since the isolated bidirectional DC DC are having more complex structure, are more bulky, costlier and heavier than the non-isolated bidirectional DC DC converters due to the presence of the transformer, they are usually unfit for the HEV application. Also the overall efficiency of the non-isolated bidirectional converters are more as compared to the isolated bidirectional converters. Therefore the Non-Isolated Half Bridge Bidirectional DC-DC converter is selected for the present design.

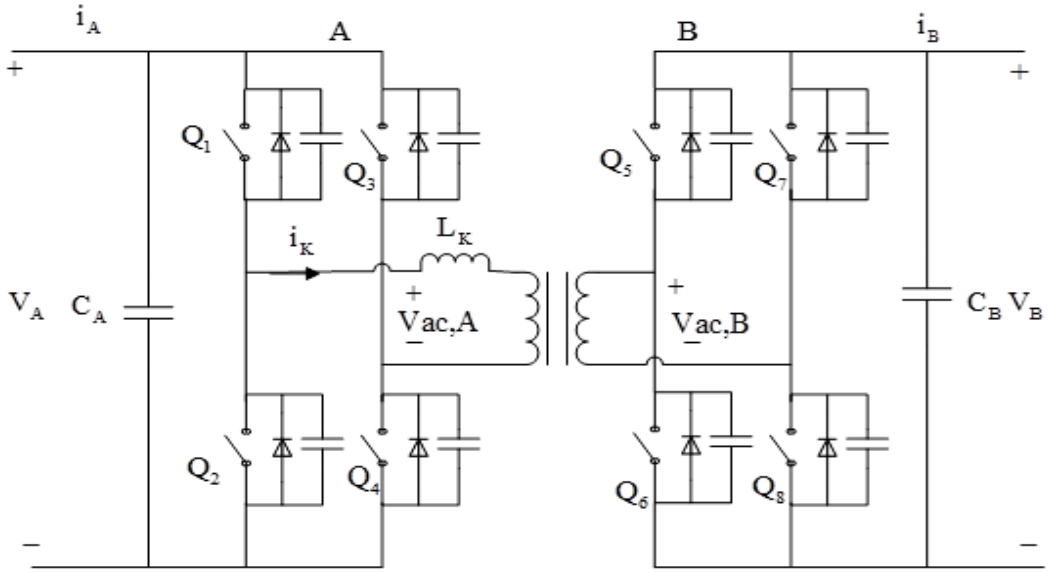

Figure 2.8: Dual Bridge Isolated Voltage Fed Bidirectional DC DC Converter

2.3 Motor selection for HEV propulsion system

Motor selection is an important part of electric vehicle design since the motor and the motor drive configuration characteristics directly influences the performance of electric vehicle. For the Vehicle propulsion system the decision for the selection of the motor type, motor drive system, battery and power control system is based on the parameters as per the design specification of the vehicle i.e. the start-up and the max torque, maximum speed, average travel range, battery capacity, overall weight and size of the system. a high instantaneous power and power density. The basic requirements of the motors to be employed for the HEV drive train are as follows [15,16]:

- high start-up torque for starting as well as climbing, and high power at high speed ;
- very wide speed range having constant-power region;
- high efficiency over the wide speed range with constant torque and constant power regions;
- fast torque response;

- high efficiency for regenerative braking;
- downsizing, weight reduction, and lower moment of inertia;
- high reliability and robustness for various vehicle operating conditions;
- reasonable cost;
- fault tolerance;

Fundamentally the motors used in hybrid electric vehicles are the same as those used for other applications except some minor modifications where the motors has to be directly used as the hub of the wheel, for e.g. generally BLDC motor are used as the hub motors. Because of the electric motors in hybrid electric drive, the torque generation is very fast and accurate. Below is the brief description of the some of the motors used in the Hybrid Electric Vehicle drive:

Brushed DC Motor

DC motor generally has electrical windings in the rotor and the stator is composed of the permanent magnet or electrical windings that act as electromagnets. The speed torque characteristics of DC motor matches the traction requirements of a vehicle, therefore they remain an attractive option. The torque is maximum at the low speed and it gradually decreases as the speed increases. Therefore it can provide good starting torque. Also the controllers for the DC motors are simpler and inexpensive. But it has a bulky construction and due to the brushed commutation, it requires periodic maintenance. At higher speeds, brush friction gets increased, and therefore the useful torque decreases. Also the power rating of the motor gets limited by the heat produced by the armature. This heat is dissipated in the air gap and thus increases the temperature in the air gap and therefore it limits the motor power and motors output frame. This is the main disadvantage of the DC motor. Rotor inertia of the DC motor is also higher which limits its dynamic characteristics.

Brushless Direct Current Motor (BLDC)

BLDC motor is an AC motor. It is also known as permanent magnet synchronous motor, electronically commutated motor etc. Since the armature has no brushes for commutation, it is called Brushless DC Motor. Commutation in BLDC motor is electronically achieved based on Hall position sensors. Few limitations of brushed motors is overcome by brushless motors, i.e. they have higher efficiencies and reduced mechanical wear and tear of the commutator assembly. Although these motors also has the parallel disadvantages that they are more expensive, less rugged, higher complexity, and expensive control electronics. Generally in a brushless motor the rotor is made up of the permanent magnets instead of the electrical windings like in a DC motor, and a fixed armature, and therefore the problem of connecting the current supply to the moving armature gets eliminated. Commutation is achieved by an electronic controller instead of a brush commutator which continuously switches the phase of the supply to the winding so the motor keeps rotating. Since no electrical windings is present on the rotor, therefore the centrifugal forces due to rotation does not acts on them and also since as they as are encased in the motor housing, the heat generated can be dissipated by the conduction through the main assembly and hence no air flow is required to cool the motor. Therefore the motors internal part can be completely enclosed and thus can be protected against foreign matters and dust.

Advantages of the BLDC motor over the DC motor are as follows:

- torque per weight and more torque per watt i.e. increase in efficiency,
- increased reliability,
- longer lifetime and no maintenance since no brush and therefore no commutator erosion,
- elimination of ionizing sparks from the commutator, and therefore the re-

duction of electromagnetic interference (EMI)

- reduced noise

Disadvantages:

- The maximum power rating of the BLDC motor is limited mainly by the heat; since excessive heat weakens the permanent magnets and damages the windings insulation.
- It has higher cost because of the complex electronic speed controllers.
- It can also be regulated by a comparatively simple controller, such as a potentiometer using variable resistor. However, this reduces efficiency since power is wasted in the resistance.

AC Induction Motor

Induction motors or an asynchronous motors are the most preferred and the potential candidate for the HEVs. Induction motor is an AC motor in which current is induced by the electromagnetic induction in the rotor winding by the magnetic field of the stator winding. Therefore they do not require the slip rings or the commutator brushes to slide on the rotor surface for the transfer of the current. Rotor windings is made up of the short-circuited loops of conductors and can be of two types :wound rotor and the squirrel cage type. It has the nonlinear speed to torque characteristics i.e lower torque at lower speeds. Since both stator and rotor have windings, the output power to size is quite lower than BLDC motors. Also the motor runs at a lower speed by an amount equals to slip frequency than the stator and the slip increases with the load. They are generally more suitable for the industrial and traction drive purposes. Also,presently the induction motor drive technology is the most advanced technology among the commutatorless motor drives.

Advantages:

- reliability,
- low maintenance,
- low cost
- ruggedness, and
- ability to operate in adverse environments.

Disadvantages:

- its efficiency is lower than the PMDC motors due to the presence of the windings in the both rotor and the stator which increases the copper losses.
- low power factor,
- low inverter usage

Switched Reluctance Motor (SRM)

It is a type of synchronous machine. IN SRM only the stator has electrical windings whereas the rotor contains no windings or permanent magnets. It consists of only steel laminations stacked onto a shaft. Both the stator and the rotor are made up of the irons and are magnetized by the current through the stator coil. The rotor motion is produced because of the variable reluctance in the air gap between the stator and the rotor. When a stator winding is energized, it produces a magnetic field, and hence reluctance torque is produced because of the tendency of the rotor is to move to its minimum reluctance position. The current in the stator coil does not need to alternate.

Advantages:

- Low Cost because of simple construction

- It can achieve very high speed as compared to other motors due of the absence of the conductor windings or permanent magnets on the rotor.
- It is very reliable since each phase of the SRM is physically, magnetically, and electrically independent from the other motor phases.

Disadvantages:

- It has be to always electronically commutated., it can not run directly from a DC bus or an AC line.
- The saliency of the stator and rotor which is necessary to produce reluctance torque, results into strong non-linear magnetic characteristics. This makes the analysis and the control of the SRMs complicated.

Selection of Motor for the Electric bicycle design

Generally low-cost electric scooters and electric bicycles, PM dc motor and PM brushless dc (PMBLDC) motors are the most used. Usually, the PMBLDC motor is used in a direct drive motorization (Hub motors) scheme and is mounted in the wheel. The simplest control method is based on an inverter with voltage control, PWM modulation and current limitation. Its optimal operating point is at low speed and high torque. The PM DC motor drive the wheel through a gear/chain and therefore due to the gear changing mechanism it may operate satisfactorily at higher speeds and lower torques. The speed control is achieved by the armature voltage variation generally by using a chopper. These low-cost structures does not incorporate any mechanism for regenerative braking control strategy. PM brushed dc motor drives are used in the lower cost traction systems. It uses a simple PWM chopper converter and a maximal current limitation without having any current control. The duty cycle is manually adjusted directly by the throttle which in turn varies the voltage between the brushes. This is a unidirectional current converter and it is not possible to implement regenerative breaking. Main advantages of this system are the cost, robustness, compactness due to possibility of reducing the motor size by using a gearbox, which allows increasing the output torque.

Typically, brush dc motors operate at high speed, up to 5000 rpm. Usually, it is a ferrite permanent magnet motor and it has low magnetic performance. Current loop control can be used for the power assisted system to amplify force applied on the pedals. The polyphase brushless dc motor produces higher torque by using high performance permanent magnets as NdFeB. Therefore, it is possible with them to realize direct-drive system in-wheel and a gearbox can thus be avoided.. The disadvantage is the increase in the complexity of the power converter and the control method. It is necessary to use a polyphase inverter. Simplified control strategy supplies each phase with square current to minimize the cost of the sensors, as current or position sensors. The controller generates only one modulation signal.

For the present design, the main idea is to use a motor which is compact, reasonably of high efficiency, should have the capability carrying the necessary load (weight of the bicycle, rider, battery, motor and other units fitted on the cycle) under ideal driving conditions. In case of extreme load conditions, for example while the bicycle is being driven up a slope, the motor should be in a position to meet it as far as possible. A motor with a constant speed characteristic will provide a sense of comfort especially while driving down steep slopes. Also, the incorporation of regeneration should be easy. All this factors makes the PMDC motor as the most appropriate for our case.

Chapter 3

Bidirectional DC DC Converter fed PMDC motor

Chapter 3

Bidirectional DC DC Converter fed PMDC motor

3.1 Bidirectional DC DC Converter fed PMDC motor Power Stage

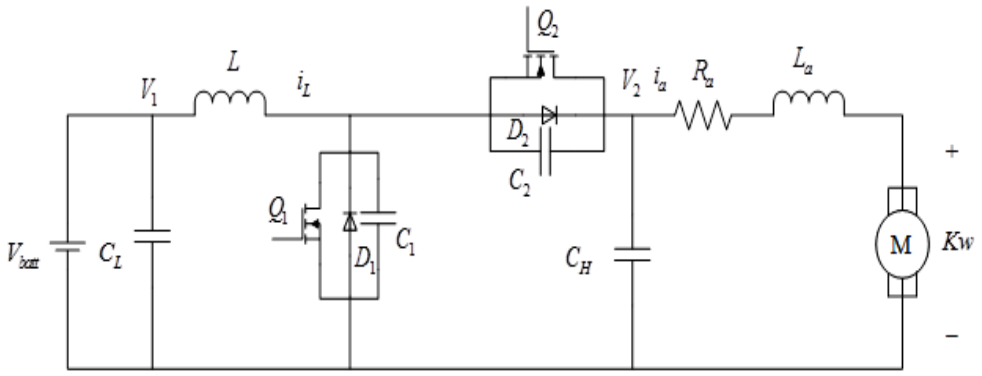

Figure 3.1: Bidirectional DC DC converter fed PMDC motor

3.1.1 Circuit Description

Converter operation: Fig 9 shows the proposed soft-switching bidirectional dc-dc converter fed PMDC motor circuit topology. The bidirectional dc-dc converter is operated in boost mode for forward motoring and in buck mode for regenerative braking of the PMDC motor. On the low-voltage side, a battery pack is placed , and on the other side a PMDC motor whose speed has to be controlled is installed. It also contains a high-frequency capacitor as the energy buffer along the motor side as well as a smoothening capacitor along the battery side.

3.1.2 Circuit specifications

The design specifications are as follows:

Parameter	Notaion	Values
Maximum converter power	P	$500W$
Battery output voltage range	$V_{BATT,OUT}$	$15V-17V$
Battery input voltage range	$V_{BATT,IN}$	$13V-16V$
DC Bus voltage	V_A	$17V-40V$
Swtiching frequency	f_S	$10kHz$
Percentage Battery discharge current ripple	$\Delta I_{BATT,OUT}$	5%
Percentage Battery charging current ripple	$\Delta I_{BATT,IN}$	20%

3.1.3 Converter Operation

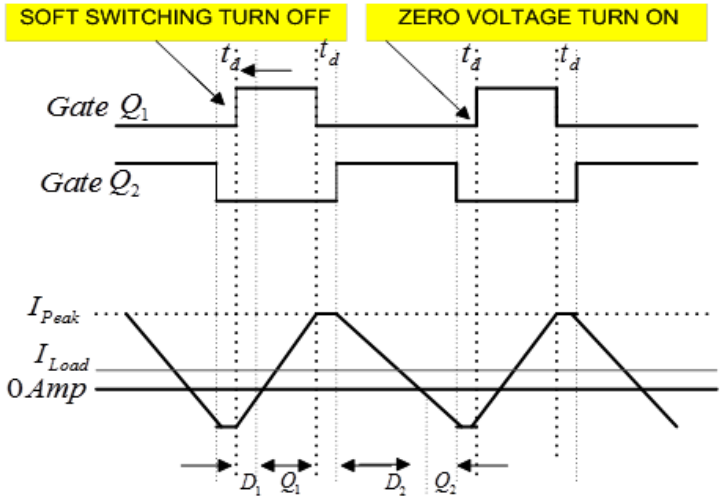

Figure 3.2: Complimentary Gate Switching for ZVRT turn on and Soft Switching turn off and inductor current

Assume that the converter is operating in the boost motoring mode with the constant speed and fixed load torque so that the motors armature voltage and the inductor current is at steady state . ZVRT soft switching technique [19] has been used here for the converter's switching operaton. Let initially the main switch Q1 is conducting as shown in the diagram and hence the inductor current rises

till not it reaches the dead time when all the devices gets turned off, and therefore the inductor current will charge the capacitor C1 and discharge C2. Due to the presence of the snubber capacitors C1 and C2 , the charging and discharging rates are reduced .Since the voltage across the capacitors cannot change abruptly, therefore the switching on and switching off losses are reduced. Now the inductor current flows through the diode D2 and decreases due to the opposition from voltage across capacitor CH till not it becomes zero and reverses its polarity through Q2, thus the switch Q2 gets on at zero voltage because of the freewheeling current through D2. Also the diode gets switched off at the zero voltage and therefore the reverse recovery losses are reduced. Again the negative inductor current goes though switch Q2 which helps in charging C2 and discharging C1 during the dead time and after that again the negative current is bypassed through diode D1 till not it becomes zero and the switch Q1 turns on. Thus the switch Q1 turns on at Zero Voltage condition.

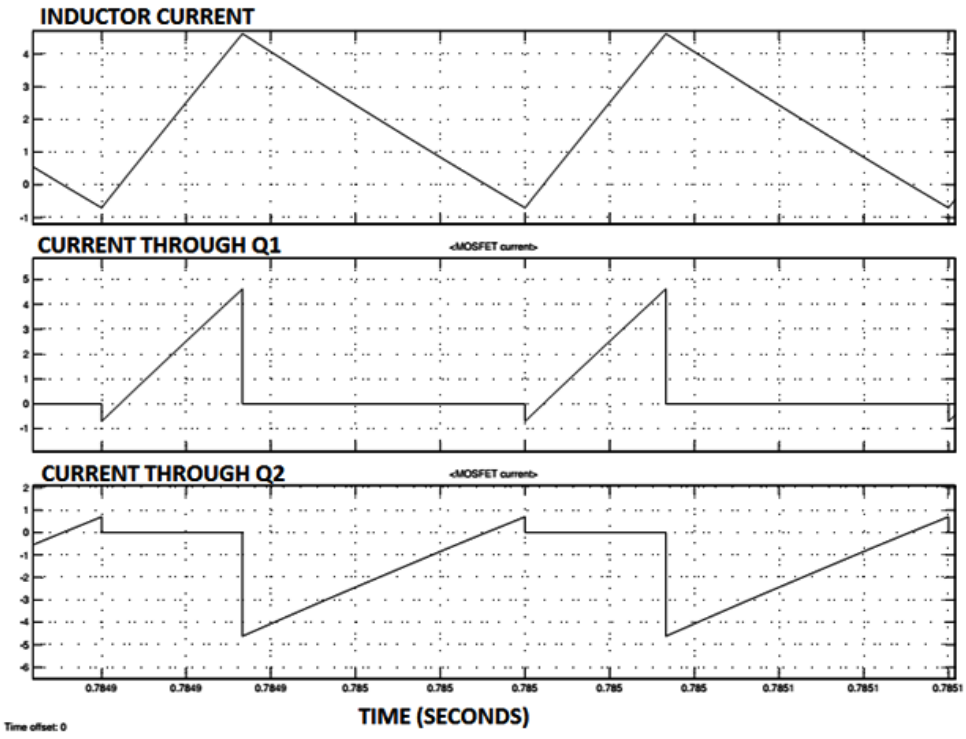

Figure 3.3: Inductor current, MOSFET Q1 current and the MOSFET Q2 current during motoring operation

3.2 Converter's Parameters Designing

The Bidirectional DC DC converter can operate in the continuous conduction mode, discontinuous conduction mode as well at the edge of continuous conduction mode and discontinuous conduction mode. The effect of converter's operation in these three conduction modes affects its efficiency and performance in different ways. Therefore converter's operation analysis in three modes is necessary before the design of the circuit parameters.

3.2.1 Converter operating in the motoring mode in continuous conduction mode

Fig 3.4 shows the converter operating in the continuous conduction mode during motoring. The converter operates in the boost mode so as to step up the battery voltage so as to provide the proper drive to the motor. In this mode is always positive I_L i.e. $I_L > 0$.

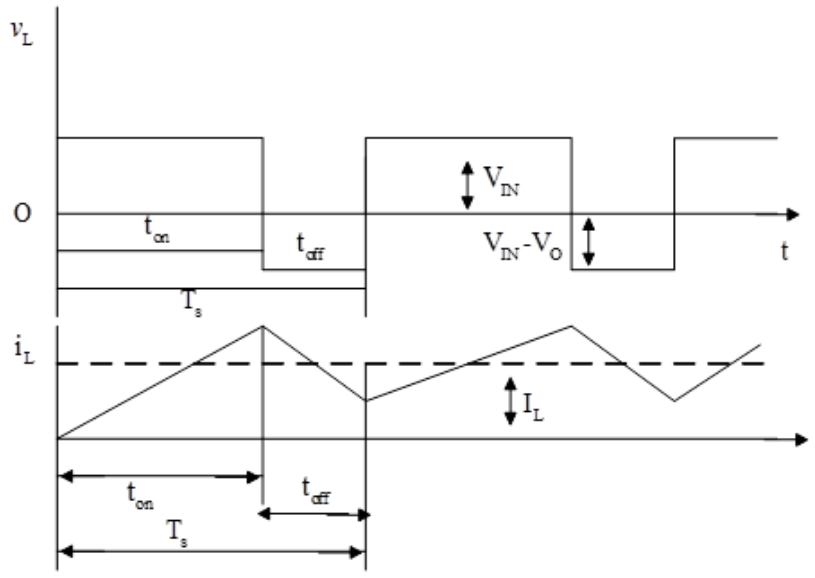

Figure 3.4: Inductor current waveform during motoring operation in continuous conduction mode

Therefore the basic equations governing the circuit operation in this mode are as follows:

$$V_{IN} t_{ON} + (V_2 - V_{IN})\, t_{OFF} = 0 \tag{3.1}$$

Dividing both the sides by the switching time period T_s and rearranging we get,

$$\frac{V_2}{V_{IN}} = \frac{1}{1-D}, \tag{3.2}$$

Assuming lossless converter operation, the power input should be equal to the power output, then

$$P_o = P_{IN} \tag{3.3}$$

$$V_2 I_A = V_{IN} I_L \tag{3.4}$$

$$\text{Therefore,} \quad I_A = I_L 1 - D \tag{3.5}$$

3.2.2 Boundary between Continuous and Discontinuous Conduction during Motoring mode

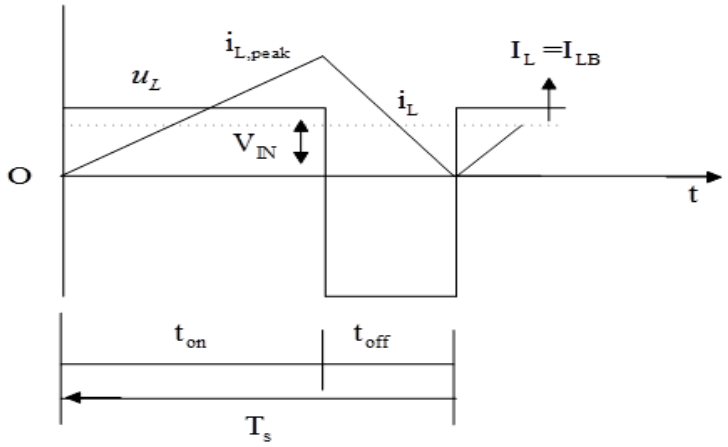

Figure 3.5: The waveforms of inductor current during motoring mode at the edge of continuous and discontinuous mode of conduction

Fig 3.5 shows the inductor waveforms at the edge of continuous conduction and discontinuous conduction mode during motoring operation. Therefore at the end of the switching period the inductor current just reaches zero. The average value of the inductor current at the boundary is given by:

$$I_{LB} = \frac{1}{2} I_{L,PEAK} = \frac{1}{2} \frac{V_{IN}}{L} t_{ON} = \frac{T_s V_2}{2L} D(1-D) \tag{3.6}$$

where I_{LB} is the average value of the inductor current at the edge of continuous and discontinuous mode of conduction.

Considering that during motoring operation(i.e. boost mode), the inductor current and the input current are the same ($I_1 = I_L$),we find that the average output current during motoring mode at the verge of continuous conduction mode is:

$$I_A = I_L(1 - D) \tag{3.7}$$

$$I_{A,AVG} = \frac{T_s V_2}{2L} D(1 - D)^2 \tag{3.8}$$

From the above equation we find that the I_{LB} reaches the maximum value at $D = 0.5$,

$$I_{LB,MAX} = \frac{T_s V_2}{8L} \tag{3.9}$$

Also I_A has its maximum value at $D = 0.33$,

$$I_{AB,MAX} = \frac{2}{27} \frac{T_s V_2}{L} = 0.74 \frac{T_s V_2}{L} \tag{3.10}$$

where I_{AB} is the average value of the armature current when the converter is operating at the verge of conduction and disconduction mode.

In terms of their maximum values, $I_{LB,MAX}$ and $I_{AB,MAX}$ can be expressed as:

$$I_{LB} = 4D(1 - D) I_{LB,MAX} \tag{3.11}$$

$$I_{AB} = \frac{27}{4} D(1 - D)^2 I_{AB,MAX} \tag{3.12}$$

3.2.3 Discontinuous Conduction Mode

Since the voltage across the inductor over one time period should be zero, therefore

$$V_{IN} D T_s + (V_{IN} - V_2) \Delta_1 T_s = 0 \tag{3.13}$$

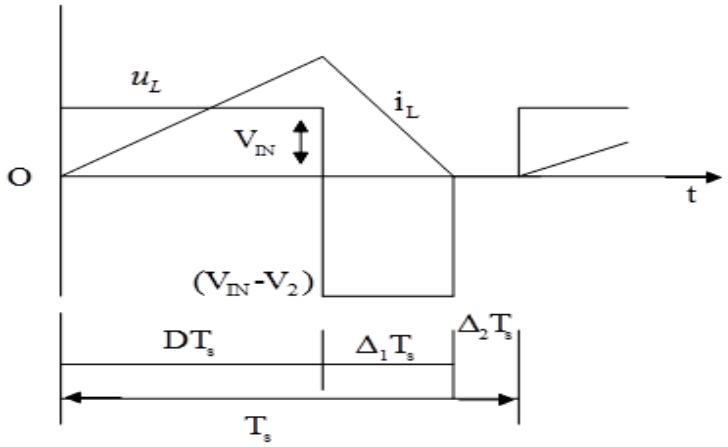

Figure 3.6: Inductor current waveform during discontinuous conduction mode

$$\text{Thus,} \quad \frac{V_2}{V_{IN}} = \frac{\Delta_1 + D}{\Delta_1}$$
$$\text{and} \quad \frac{I_A}{I_{IN}} = \frac{\Delta_1}{\Delta_1 + D} \tag{3.14}$$

From the above Fig 3.6, average battery current(input current) , which is also equal to the average inductor current therefore,

$$I_1 = \frac{V_{IN}}{2L} DT_s(D + \Delta_1) \tag{3.15}$$
$$I_A = \frac{T_s V_{IN}}{2L} D\Delta_1 \tag{3.16}$$

If V_2 is regulated so as to run the motor at the constant speed and the load is varying, then the motor current is going to vary so as to so provide the required torque. We can get the expression of motor current in terms of the duty cycle with the armature voltage constant as:

$$D = \left[\frac{4}{27}\frac{V_2}{V_{IN}}\left(\frac{V_2}{V_{IN}} - 1\right)\frac{I_A}{I_{A,MAX}}\right]^{\frac{1}{2}} \tag{3.17}$$

3.2.4 DCM operation of the Converter

Bidirectional DC DC converter are generally operated in the continuous conduction mode (CCM), and hence its design requires a larger valued filter inductor. A larger inductance can result in an increase in physical size of the inductor, which is not desirable. This large filter inductor can also slow down the transient response

of the converter as well as slow down any type of mode transitioning.With the circuit operating in the discontinuous conduction mode(DCM), the inductor value considerably reduces . Since the DCM operation facilitates the minimization of the inductor value and thus making the response faster, therefore the converter can designed to have a high power density by operating in DCM mode. Another significant advantage is the zero-turn on loss and therefore low reverse recovery loss in diode during DCM operation. But, since in the DCM operation the main switch is switched off at double the value of the load current, therefore the losses during turn off increases. Also because of this , the inductor current exhibits parasitic ringing during turning off of the switch since the output capacitance of the switch in association with the inductor tries to oscillate and hence causes power dissipation and electrical stresses on the devices. This is the major disadvantage associated with the DCM operation. The efficiency reduces because of all this negative effects of the DCM operation. Therefore the soft switching techniques as well as the remedial measures for the parasitic ringing have to be ensured in the converter design.

3.3 Soft Switching Methods

If the converter circuit does not have any auxiliary components , then the switches operates under hard switching operation and this leads to the considerable amount of the power loss and high electrical stress within the switches during turn on and turn off condition because of very large values of the current and voltage simultaneously across it. Generally in all the converters operating under hard switching conditions and particularly in the high power converters, switching losses puts the major limitation on the increase of the switching frequency which is desired for the reduction in components values and hence the size cost and the compactness of the converter. Therefore a compromise is made with the value of the switching frequency in the practically acceptable range so as to achieve the high efficiency in the converter and at the same time to and limit its cost. The reduction in the value of the switching frequency increases the

size of the passive components such as the capacitors, inductors, transformers etc and makes the DC DC converter heavier and bulky. Soft switching techniques when employed for the power converters, helps in increasing energy conversion efficiency , shifts up the upper limit for increasing switching frequency and thereby the reduction in the size ,weight and the cost of the passive components as well as the reduction of the electrical and thermal stresses along the switching devices and the EMI reduction during switching. Thus the power loss during switching is eliminated from the converter. Soft switching can be achieved by the addition of the resonant components (snubber capacitor or inductor) or else by the use of the parasitic component of the converter circuit. Soft switching is realized in the DC DC converters circuit by the addition of the resonant switches consisting of a controlled semiconductor switch (power MOSFET or an IGBT), an antiparallel external diode and a resonant capacitor or a resonant inductor. Here the Soft switching can be achieved by the either zero voltage or zero current switching condition. The condition of soft switching can only be realized in the converter circuit if the resonant part of the switch has the capability to reset itself (i.e. discharge itself) at the time of switching. If the resonant capacitor or the inductor across the switches can discharge themselves and thereby acquire zero voltage of zero current at the time of the switching, soft switching is established. Thus by the addition of the external circuit elements, the circuit can be made to operate under soft switching condition.

3.3.1 Zero current switching

For achieving the ZCS condition in the switch, a resonant inductor L_R is added in series along the controlled semiconductor switch as shown in the fig 3.7.

When the switch is at the off state, there is zero current through the inductor. At the time of the transition of switch state, since the current through the inductor cannot rise instantaneously, therefore the inductor charging rate is decreased and a very low inductor current flows till not the voltage across the switch decreases appreciably to the on state value. Hence a very low power is dissipated during

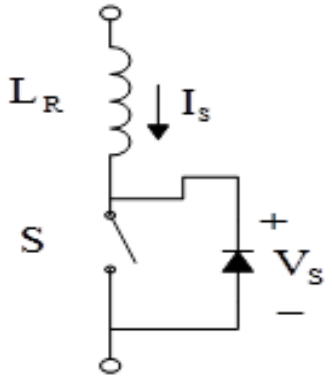

Figure 3.7: An elementary resonant switch for achieving ZCS

switching operation. The ZCS turn off across the switch is obtained by the resonance operation of the L_R with an external capacitor connected with the switch. External capacitor can be connected in parallel or series depending up on the circuit topology. During the resonance transition, the current decreases to zero and the ZCS is established. During resonance transition, since the voltage across the capacitor cannot change instantly, therefore the charging rate of the capacitor is reduced and the current decreases appreciably before the voltage across the switch starts rising. Thus ZCS is achieved.

3.3.2 Zero Voltage switching

ZVS condition in the switch can be realized by the switch parasitic capacitance or by a resonant capacitor C_R is added in parallel across the controlled semiconductor switch as shown in the Fig 3.8.

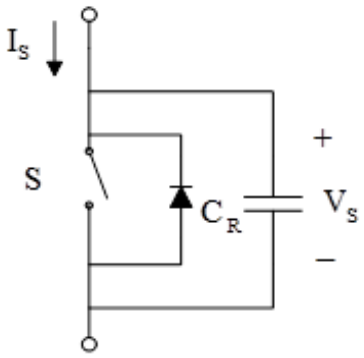

Figure 3.8: An elementary resonant switch for achieving ZVS

When the switch is in the on state, the capacitor is having the voltage equivalent to the forward voltage of the switch. At the time of the transition of switch state, since the voltage across the capacitor cannot change instantaneously, therefore the capacitor charging rate is decreased and hence the current almost falls to zero (off state current) till not the voltage across the switch starts increasing to that of the off state value. Hence a very low power is dissipated during switching turn off operation. The ZVS turn on is obtained by the resonance operation of the C_R with an external inductor connected with the switch either in parallel or series depending up on the circuit topology. Because the resonance transition, the current starts increasing after the voltage drops down to zero and the hence ZVS is established. During resonance transition, since the current through the inductor cannot change instantly, therefore the charging rate of the inductor is reduced and the voltage decreases appreciably before the current across the switch starts rising. Thus ZVS is realized.

The output parasitic capacitance of the semiconductor switching devices itself can be used for achieving the ZVS operation except for the conditions when there is a limitation put up by the dead time period during switching during which the resonance charging and discharging takes place. In those conditions, external resonant components have to be used for achieving ZVS condition.

3.4 Parasitic Ringing Due To Parasitic Capacitance

Although a smaller inductor can be used to achieve DCM operation, there is an inherent problem in high power bidirectional converters. This problem is the parasitic ringing caused by the converters inductor and the power device parasitic capacitances. In high power applications, the major power device being used is IGBT module, whose output capacitance is much larger than that of discrete power device, thus large capacitance will have an impact on converter performance [21]. The circuit in Figure 1 shows the boost converters critical loop created by

the parasitic inductances and capacitances, labelled as L_{PAR} and C_{PAR} reference designators.

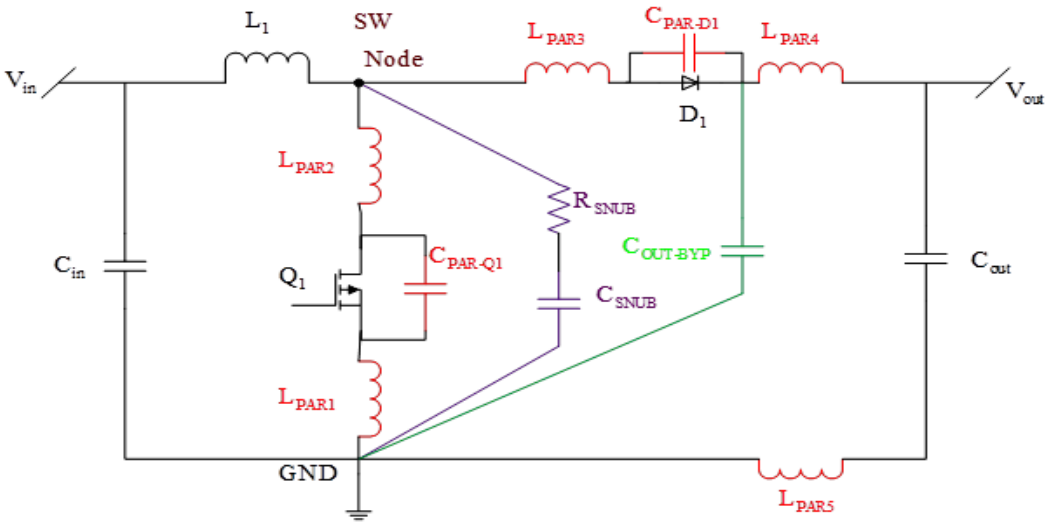

Figure 3.9: Parasitic inductance and capacitance in a boost converter

The node where the two switches and inductor of a switching converter meet is called the switch node. It is not uncommon for the parasitic inductances and capacitances to interact and cause voltage oscillations. If the amplitude of this ringing is above the absolute maximum rated voltage of the low-side switch, it can be destructive to the switch. In addition, the conducted emissions and/or electromagnetic interference (EMI) generated by the ringing can cause problems for any nearby ICs. The device parasitic capacitance tends to ring with the boost inductor when high frequency voltage is applied to it. The frequency of ringing and the magnitude of the oscillating current, both are functions of the inductance and the parasitic capacitance of the device, which are as shown in the equations below :

$$f_{RINGING} = \frac{1}{2\pi\sqrt{LC}} = \frac{1}{2\pi\sqrt{2LC_{PAR}}} \tag{3.18}$$

In order to reduce the effect of ringing the power switches and diodes with minimal parasitic capacitances should be selected. As the converters inductor

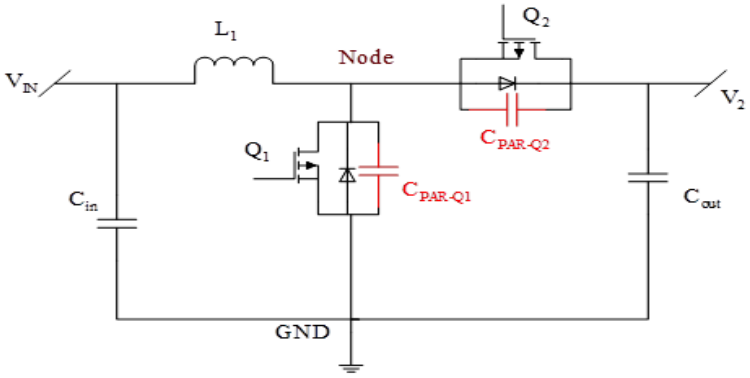

Figure 3.10: Non-Isolated Bidirectional DC DC Converter Parasitic Capacitances

resonates with parasitic capacitance of the device, the maximum circulation energy can be calculated as shown below:

$$E_{CIRCULATION} = 2 \times \frac{1}{2} C_{PAR}(V_2 - V_{IN})^2 = C_{PAR}(V_2 - V_{IN})^2 \tag{3.19}$$

This circulation energy will be dissipated as two parts, one part will be dissipated as proximity effect on inductor winding, resulting in copper loss, and another part will be dissipated during device turn-on as turn-on loss. At the high ringing frequency, the ac resistance of the inductor winding will increase significantly due to skin effect and the proximity effect will appear as well due to the multilayer winding structure made by copper coil. Therefore it can be seen that the circulation energy has to be reduced to improve converter efficiency by reducing the parasitic capacitance of the device. When the converters inductance is fixed with a larger device, the ringing frequency is lower, but the magnitude will be higher and the copper loss will be higher due to this high frequency ringing current.

3.5 Inductance Selection

A major design aspect in a high power converter is the selection of the inductor. The design of the inductors plays a crucial role in the overall converter operation. The major concern here is the size and weight of such a high power inductor that is perhaps the single heaviest component in the entire converter. A small inductance value is preferred in order to reduce the inductor size and weight. A criterion that

is simple but reasonable is to have the full (rated) load current operating under DCM/CCM boundary condition. Other load conditions will have smaller inductor current under DCM operation.

The equations defining the inductor current during motoring in the DCM mode are as follows:

The minimum inductance value needed to insure the converter operates in CCM is known as the critical inductance value. For the buck and boost converter the critical inductance value is dependent on the steady state duty cycle, switching period and the load resistance. The equation for the critical inductance for the boost converter is given by:

$$L_{CR,BOOST} = \frac{T_s R_{LOAD}}{2}(1-D)^2 D \tag{3.20}$$

or the above equation can be also written as

$$L_{CR,BOOST} = \frac{1}{2}\frac{V_2 - V_{IN}}{P}\frac{V_{IN}^2}{V_2}T_s \tag{3.21}$$

Similarly the critical inductance for the buck mode CCM operation is given by

$$L_{CR,BUCK} = \frac{(1-D)V_2}{2I_A}T_s \tag{3.22}$$

Therefore the value of the converter inductor should be less than the value given by

$$L = min\left[\left(\frac{1}{2}\frac{V_2 - V_{IN}}{P}\frac{V_{IN}^2}{V_2}T_s\right), \left(\frac{(1-D)V_2}{2I_A}T_s\right)\right] \tag{3.23}$$

Also the output and input capacitor values found from the capacitors voltage ripple are given as below:

$$C_1 = \frac{\Delta I}{8\Delta V_{IN}}T_s \tag{3.24}$$

$$C_2 = \frac{V_2 D}{R_A \Delta V_2}T_s \tag{3.25}$$

Also the inductor ripple current is given by the equation

$$\Delta I = \frac{1}{2}\frac{V_2 - V_1}{L_C}\frac{V_1}{V_2}T_s \tag{3.26}$$

And the inductor current is given by

$$I_{RMS} = \sqrt{I_{Load}^2 + \frac{\Delta I^2}{3}} \tag{3.27}$$

If the motors rated power is given by,

$$P_{M,RATED} = V_{M,RATED} \cdot I_{M,RATED} \tag{3.28}$$

where $V_M = V_A = V_2$and $I_M = I_A$, then

$$I_A = \frac{P_{M,RATED}}{V_2} \tag{3.29}$$

Also we know that

$$I_{Min} = I_{Load} - \Delta I \tag{3.30}$$

$$\text{and} \quad I_{Peak} = I_{Load} + \Delta I \tag{3.31}$$

If P is the maximum power rating for which the converter is to be designed then, the inductance value for which the inductor current will be just in the edge of the DCM mode while at rated power is given by:

$$L_{CR} = \frac{1}{2}\frac{V_2 - V_{IN}}{P}\frac{V_{IN}^2}{V_2}T_s \tag{3.32}$$

Putting the value of we get

$$I_{Min} = I_{Load} - \frac{1}{2}\frac{V_2 - V_1}{L_C}\frac{V_1}{V_2}T_s \tag{3.33}$$

$$I_{Peak} = I_{Load} + \frac{1}{2}\frac{V_2 - V_1}{L_C}\frac{V_1}{V_2}T_s \tag{3.34}$$

In our case $V_2 = 25V,\ V_1 = 15V,\ T_s = 100\mu s,\ I_{Load} = 2.131A$

With the above values, plotting the graph for L versus I_{Min} and L versus I_{Peak} , we get

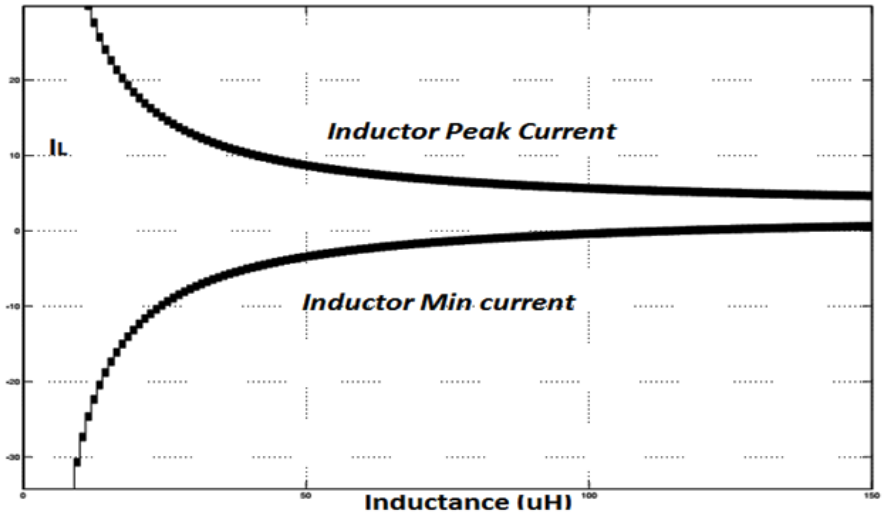

Figure 3.11: Inductor Value Optimization for DCM operation

From the graph we see that at the inductance value of $L = 100\mu H$, the inductor current reaches the negative value, therefore we select the converter inductor value equals $L = 100\mu H$.

Chapter 4

State Space Modeling and Controller design

Chapter 4

State Space Modeling and Controller design

4.1 Introduction

The design and optimization of motor fed DC DC converter power stage circuit parameters were shown in the previous chapter. In this chapter, the power stage modelling is described and the circuit parameters are introduced. In section 4.2, the necessary assumptions have been made for modeling, and consequently the system model has been developed in section 4.3 on the basis of the state space averaging method . The general-purposed power stage model can be used under different operating modes. It is assumed that there exists two dc sources including motors back EMF voltage K_w along high voltage side and low voltage side battery source V_{IN}, constituting the voltage sources on the both the sides of the bidirectional dc-dc converter. With two voltage sources, the averaged inductor current I_L or averaged output current I_A can flow in both directions, instead of flowing only in one direction in one voltage source application . Motor's armature resistance R_A represents either high-side source internal resistance during motoring mode (charging) and regenerative mode (discharging) or as a load in motoring(boost) mode. Resistor R_1 is the internal resistance of the source battery for both for modes or it acts as load during regeneration(buck) operation. Capacitor C_L and C_H represents the capacitor bank of the battery and the output capacitor at motor side respectively. Two active switches Q1 and Q2 are controlled by complementary gating control signal Gate1 and Gate2 separately.

The switch Q_1 is the control switch during motoring. Inductor parasitic resistance R_{LP} and MOSFET turn-on resistance R_{DSON} are neglected in the model. System consists of four energy storage components i.e. input capacitor $C_1 = 5\mu F$, output capacitor $C_2 = 2.88mF$, converter's inductor $L = 100\mu H$ and the motors armature inductance $L_A = 28mH$, also motor acts as an electromechanical transducer for changing the electrical energy into mechanical energy (load torque). Further we have motor's moment of inertia $J = 0.05215kg.m^2$, viscous friction coefficient $B_m = 0.002953N.m.s$, motor's armature resistance $R_a = 1.4\Omega$, motor's torque constant $K = 0.5N.m.A^{-1}$, and load torque $T_L = 0.5N.m$. Also we have battery voltage $V_{batt} = 15V$, battery's internal resistance $R_1 = 0.025\Omega$ and converter's nominal duty ratio $D = 0.4$.

4.2 Model Assumptions

Following assumptions are made before the state-space averaging method is employed for the modeling of the bidirectional dc-dc converter. The validity of the assumptions can be verified from the simulation results, which were in agreement with the assumptions made in our case.

Small Ripple Assumption: The inductor ripple current is assumed to be low enough so that the state space averaging can be applied. This assumption can be verified by comparing the simulating output with the output of the averaged model.

Negligible Dead-Time Effect: The switching period is 100 microsecond i.e 10kHz whereas the dead time period of 1 microsecond is selected. Thus the dead time is only approximately 1 percent of the total period, and it can be neglected. Following the same analogy, we can also omit the soft switching period.

Identical Voltage Drop across devices during conduction in both the modes: Since the device conduction voltage drops is very small as compared to

the DC bus voltage, therefore the variation in voltage drop among the identical devices will even be much smaller than this fraction. Therefore , we can easily neglect the voltage drop variations during the power flow in the different directions.

4.3 State-space Averaged Model

As we have already discussed about the circuit operation in the chapter 2 and 3, it can be easily inferred that no matter the circuit is in either operating modes, whether motoring or regenerative mode, there are always two subintervals t_{on} and t_{off} as shown in Fig.4.1. Therefore we do not require to analyse the circuit separately during motoring mode i.e. in boost mode and the regenerative mode i.e. buck mode. Rather a simple analysis during the subintervals ton and toff will suffice for both the modes of operation.

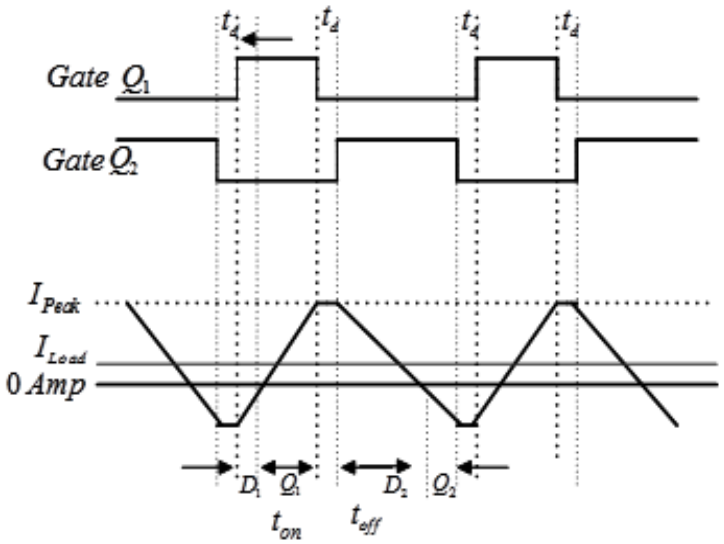

Figure 4.1: Complimentary Gating Signal Control

In the first subinterval, when the switch Q1 is on and Q2 is off, the converter equivalent circuit can be represented in Fig.4.2.

There are four energy storage components , inductor currents I_L, I_A, and the .battery side capacitor voltage V_1 and motor side capacitor voltage V_2 and the

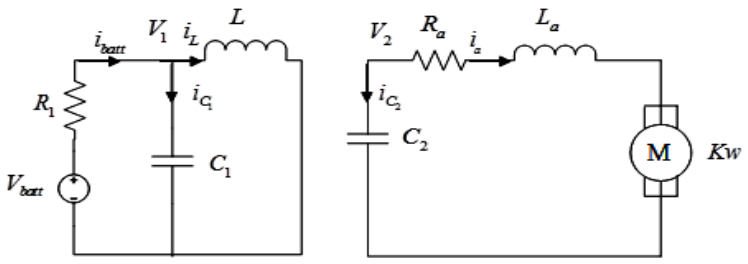

Figure 4.2: Equivalent circuit with Q1-on, Q2-off

Inductor voltage across the inductor L is given by

$$V_1 = L\frac{di_L}{dt}$$

$$\Rightarrow \frac{di_L}{dt} = \frac{V_1}{L} \tag{4.1}$$

Similarly the voltage across the armature inductance is given by

$$V_2 = i_A R_A + L_A\frac{di_A}{dt} + Kw$$

$$\Rightarrow \frac{di_a}{dt} = -\frac{R_a}{L_a}i_a + \frac{V_2}{L_a} - \frac{K}{L_a}w \tag{4.2}$$

Also the capacitor currents i_{C_1} and i_{C_2} are given by

$$V_{batt} = R_1 i_{batt} + V_1$$

$$i_{C_1} = C_1\frac{di_{V_1}}{dt}$$

$$i_{batt} = i_L + i_{C_1}$$

Therefore,

$$\frac{dV_1}{dt} = \frac{V_{batt}}{R_1 C_1} - \frac{i_L}{C_1} - \frac{V_1}{R_1 C_1} \tag{4.3}$$

$$\frac{dV_2}{dt} = -\frac{i_a}{C_2} \tag{4.4}$$

Finally the motor torque equation is given by

$$\frac{dw}{dt} = \frac{K}{J}i_a - \frac{B_m}{J}w - \frac{T_L}{J} \tag{4.5}$$

Therefore the state space equations for the first interval t_{ON} are as follows

$$\dot{X} = A_{ON}X + B_{ON}U$$
$$Y = C_{ON}X + E_{ON}U \tag{4.6}$$

Where,

$$X = \begin{bmatrix} i_L \\ i_a \\ V_1 \\ V_2 \\ w \end{bmatrix}, \; U = \begin{bmatrix} V_{batt} \\ T_L \end{bmatrix}, \; Y = \begin{bmatrix} i_L \\ i_a \\ V_1 \\ V_2 \\ w \end{bmatrix},$$

$$A_{ON} = \begin{bmatrix} 0 & 0 & 1/L & 0 & 0 \\ 0 & -R_a/L_a & 0 & 1/L_a & -K/L_a \\ -1/C_1 & 0 & -1/R_1C_1 & 0 & 0 \\ 0 & -1/C_2 & 0 & 0 & 0 \\ 0 & K/J & 0 & 0 & -B_m/J \end{bmatrix}, \; B_{ON} = \begin{bmatrix} 0 & 0 \\ 0 & 0 \\ 1/R_1C_1 & 0 \\ 0 & 0 \\ 0 & -1/J \end{bmatrix},$$

$$C_{ON} = \begin{bmatrix} 1 & 0 & 0 & 0 & 0 \\ 0 & 1 & 0 & 0 & 0 \\ 0 & 0 & 1 & 0 & 0 \\ 0 & 0 & 0 & 1 & 0 \\ 0 & 0 & 0 & 0 & 1 \end{bmatrix}, \; E_{ON} = \begin{bmatrix} 0 & 0 \\ 0 & 0 \\ 0 & 0 \\ 0 & 0 \\ 0 & 0 \end{bmatrix}$$

In the second subinterval, when the switch Q1 is on, and Q2 is off, the converter equivalent circuit can be represented in Fig.4.3.

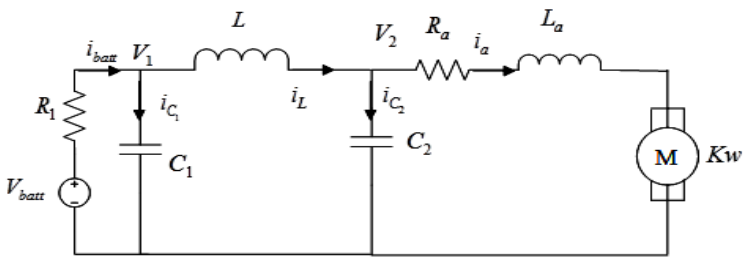

Figure 4.3: Equivalent circuit with Q1-off, Q2-on

Inductor voltage across the inductor L is given by

$$V_1 - V_2 = L\frac{di_L}{dt}$$

$$\Rightarrow \frac{di_L}{dt} = \frac{V_1 - V_2}{L} \tag{4.7}$$

Similarly the voltage across the armature inductance is given by

$$V_2 = i_A R_A + L_A\frac{di_A}{dt} + Kw$$

$$\Rightarrow \frac{di_a}{dt} = -\frac{R_a}{L_a}i_a + \frac{V_2}{L_a} - \frac{K}{L_a}w \tag{4.8}$$

Also the capacitor currents i_{C_1} and i_{C_2} are given by

$$V_{batt} = R_1 i_{batt} + V_1$$

$$i_{C_1} = C_1\frac{di_{V_1}}{dt}$$

$$i_{batt} = i_L + i_{C_1}$$

Therefore,

$$\frac{dV_1}{dt} = \frac{V_{batt}}{R_1 C_1} - \frac{i_L}{C_1} - \frac{V_1}{R_1 C_1} \tag{4.9}$$

$$\frac{dV_2}{dt} = \frac{i_L}{C_2} - \frac{i_a}{C_2} \tag{4.10}$$

Finally the motor torque equation is given by

$$\frac{dw}{dt} = \frac{K}{J}i_a - \frac{B_m}{J}w - \frac{T_L}{J} \tag{4.11}$$

Therefore the state space equations for the second interval t_{OFF} are as follows

$$\dot{X} = A_{OFF}X + B_{OFF}U$$

$$Y = C_{OFF}X + E_{OFF}U \tag{4.12}$$

Where,

$$A_{ON} = \begin{bmatrix} 0 & 0 & 1/L & -1/L & 0 \\ 0 & -R_a/L_a & 0 & 1/L_a & -K/L_a \\ -1/C_1 & 0 & -1/R_1C_1 & 0 & 0 \\ 1/C_2 & -1/C_2 & 0 & 0 & 0 \\ 0 & K/J & 0 & 0 & -B_m/J \end{bmatrix}, \quad B_{ON} = \begin{bmatrix} 0 & 0 \\ 0 & 0 \\ 1/R_1C_1 & 0 \\ 0 & 0 \\ 0 & -1/J \end{bmatrix},$$

$$C_{ON} = \begin{bmatrix} 1 & 0 & 0 & 0 & 0 \\ 0 & 1 & 0 & 0 & 0 \\ 0 & 0 & 1 & 0 & 0 \\ 0 & 0 & 0 & 1 & 0 \\ 0 & 0 & 0 & 0 & 1 \end{bmatrix}, \quad E_{ON} = \begin{bmatrix} 0 & 0 \\ 0 & 0 \\ 0 & 0 \\ 0 & 0 \\ 0 & 0 \end{bmatrix}$$

4.3.1 State-Space Averaging

During each subinterval, since all the circuit parameters are constant, therefore equivalent circuit of the converter acts like a timeinvariant system. But during switching between the two modes , the converter behaves like a time variant system. Therefore the state space averaging is used with respect to the corresponding time periods of both the subintervals so as to approximate the converter to the continuous time nonlinear time invariant system. After this, the nonlinear system is linearized about the operating point so as to get the continuous time linear time invariant system.

The two linear systems during the each subinterval are first averaged with respect to their duration in the switching period:

$$\begin{aligned} \frac{dx(t)}{dt} &= \left(d(t)A_{ON} + (1 - d(t)A_{OFF})\right) x(t) + \left(d(t)B_{ON} + (1 - d(t)B_{OFF})\right) u(t) \\ y(t) &= \left(d(t)C_{ON} + (1 - d(t)C_{OFF})\right) x(t) + \left(d(t)E_{ON} + (1 - d(t)E_{OFF})\right) u(t) \end{aligned} \tag{4.13}$$

Eq (4.1) represents the approximation of the time-variant system. The duty cycle, $d(t)$, is an additional input signal in (4.1). Therefore a new input vector is defined as.

$$u'(t) = \begin{bmatrix} u(t) \\ d(t) \end{bmatrix} \tag{4.14}$$

A nonlinear time-invariant system with state vector $x(t)$, input vector $u'(t)$, and output vector $y(t)$, can be written as

$$\begin{aligned} \frac{dx(t)}{dt} &= f\left(x(t, u'(t)\right) \\ y(t) &= g\left(x(t, u'(t)\right) \end{aligned} \tag{4.15}$$

Apply linearization method, where the deviations at operating point can be applied as follows:

$$\begin{aligned} x(t) &= X + \hat{x}(t) \\ u'(t) &= U' + \hat{u}'(t) \\ y(t) &= Y + \hat{y}(t) \end{aligned} \tag{4.16}$$

The operating-point (dc, steady-state) is denoted by capital letters and perturbation (ac) signals are denoted by the hat-symbol ($\hat{}$). Assuming that the operating point is at equilibrium point, i.e.

$$f\left(x(t), u'(t)\right) \mid_{\substack{x(t) = X \\ u'(t) = U'}} = 0 \tag{4.17}$$

The operating point output values are

$$Y = f\left(x(t), u'(t)\right) \mid_{\substack{x(t) = X \\ u'(t) = U'}} \tag{4.18}$$

The following linearized (ac, small-signal) system can now be obtained from (4.3) (Goodwin, Graebe and Salgado, 2001, Section 3.10) :

$$\begin{aligned} \frac{d\hat{x}(t)}{dt} &= A'\hat{x}(t) + B'\hat{u}'(t) \\ \hat{y}(t) &= C'\hat{x}(t) + D'\hat{u}'(t) \end{aligned} \tag{4.19}$$

Where

$$A' = \left[\frac{\partial f}{\partial x}\right]_{\substack{x(t)=X \\ u'(t)=U'}}$$
$$B' = \left[\frac{\partial f}{\partial u'}\right]_{\substack{x(t)=X \\ u'(t)=U'}}$$
$$C' = \left[\frac{\partial g}{\partial x}\right]_{\substack{x(t)=X \\ u'(t)=U'}}$$
$$E' = \left[\frac{\partial g}{\partial u'}\right]_{\substack{x(t)=X \\ u'(t)=U'}} \tag{4.20}$$

Eq.(4.19) represents an approximation for the nonlinear system.

$$u'(t) = \begin{bmatrix} u(t) \\ d(t) \end{bmatrix} = \begin{bmatrix} U \\ D \end{bmatrix} = \begin{bmatrix} \hat{u}(t) \\ \hat{d}(t) \end{bmatrix} \tag{4.21}$$

$$d'(t) = 1 - d(t)$$
$$D' = 1 - D \tag{4.22}$$

At operating point eq. (4.17) and (4.18) are written using with eq. (4.13)

$$0 = AX + BU$$
$$Y = CX + EU \tag{4.23}$$

where

$$A = DA_1 + D'A_2$$
$$B = DB_1 + D'B_2$$
$$C = DC_1 + D'C_2$$
$$E = DE_1 + D'E_2 \tag{4.24}$$

Solving eq. (4.23) for X and Y

$$X = -A^{-1}BU$$
$$Y = \left(-CA^{-1}B + E\right)U \tag{4.25}$$

$$
\begin{aligned}
A' &= A \\
B' &= \left[\frac{\partial f}{\partial u} \quad \frac{\partial f}{\partial d}\right]_{\substack{x(t)=X \\ u'(t)=U'}} = \Big[B \quad (A_1 - A_2)X + (B_1 - B_2)U\Big] = \Big[B \quad B_d\Big] \\
C' &= C \\
E' &= \left[\frac{\partial f}{\partial u} \quad \frac{\partial f}{\partial d}\right]_{\substack{x(t)=X \\ u'(t)=U'}} = \Big[E \quad (C_1 - C_2)X + (E_1 - E_2)U\Big] = \Big[E \quad E_d\Big]
\end{aligned} \tag{4.26}
$$

Eq. (4.19) becomes

$$
\begin{aligned}
\frac{d\hat{x}(t)}{dt} &= A\hat{x}(t) + B'\hat{u}'(t) \\
\hat{y}(t) &= C\hat{x}(t) + D'\hat{u}'(t)
\end{aligned} \tag{4.27}
$$

Applying Laplace Transform to above equation

$$
\begin{aligned}
\hat{x}(s) &= (sI - A)^{-1}B'\hat{u}'(s) \\
\hat{y}(s) &= C\hat{x}(s) + E'\hat{u}'(s)
\end{aligned} \tag{4.28}
$$

4.3.2 Extracting the Transfer functions

We can extract all the Transfer functions from above equation but we required only control to output function only. Therefore, control to output transfer functions is:

$$
\frac{\hat{w}}{\hat{d}} = \frac{-s^2 + \left(\frac{V_2(1-D)}{I_L L} - \frac{1}{R_1 C_1}\right)s + \left(\frac{V_2(1-D)}{I_L R_1 C_1 L} - \frac{1}{C_1 L}\right)}{s^5 + a_4 s^4 + a_3 s^3 + a_2 s^2 + a_1 s^1 + a_0} \tag{4.29}
$$

Here,

$$
\begin{aligned}
a_0 &= \left[\frac{(K^2 + B_m R_a)(1-D)^2}{R_1 C_1 C_2 J L L_a}\right] \\
a_1 &= \left[\frac{(B_m(L + L_a) + (K^2 + B_m R_a)(C_1 + C_2)R_1)(1-D)^2 (K^2 + B_m R_a) C_2 R_1 + J R_1}{R_1 C_1 C_2 J L L_a}\right] \\
a_2 &= \left[\frac{(L_a C_2 R_1 + B_m L R_1 C_1 + J L)(1-D)^2 (B_m L_a R_1 C_1 + R_a L R_1 C_1 + J L)}{R_1 C_1 C_2 J L L_a} + \frac{K^2 B_m R_a}{R_1 C_1 J L_a}\right] \\
a_3 &= \left[\frac{1}{C_1 L} + \frac{1}{C_2 L_a} + \frac{(K^2 + B_m R_a)}{J L_a} + \left(\frac{B_m L_a + R_a J}{R_1 C_1 J L_a}\right) + \frac{(1-D)^2}{C_2 L}\right] \\
a_4 &= \left[\left(\frac{B_m L_a + R_a J}{J R_a}\right) + \frac{1}{R_1 C_1}\right]
\end{aligned}
$$

4.4 Controller design for speed control of PMDC motor fed by Bidirectional DC DC converter:

The averaged state space model of the power stage developed above allows us to analyse the stability and the control issues related to the circuit. Generally the transfer function of the unidirectional power flow in normal buck or boost mode is easily known, but in the present case there is only one transfer function for the power flow in both the modes i.e. motoring as well as regeneration. Therefore the power flow depends upon the duty cycle and the instantaneous voltage across both the sides. Since the voltage of the battery is generally fixed, the voltage variation only exists at the input of the motor terminal i.e armature voltage and this depends on the back emf of the motor and the duty cycle. The power can flow in both the directions in the bidirectional dc dc converter in all the three modes as discussed in section 3.2 depending on the armature voltage and the duty cycle. Also the transition between the motoring and the regeneration mode can also be estaiblished.

The smooth transition control during the power flow in the bidirectional dc-dc converter also requires different considerations in different modes. In the present case we have two operating modes ie motoring as well as regeneration and the and the power flow in both the mode requires:

1. wide range output voltage regulation for wide range of the speed tracking.
2. wide range current regulation with almost constant voltage during regenerative braking for buck operation.

For electric vehicle, the power management needs boost power discharging mode. At the time of startup or during acceleration, battery must provide more power for the motor driving. Therefore we can actually control the power for the voltage and current regulation in both the modes . Considering almost constant motor current for the fixed load , the power flow control also means the voltage control. Therefore voltage regulator is needed for motoring mode at constant speed. Since

in a dc motor , the speed is directly proportional to the armature voltage, whereas the the torque is directly proportional to the armature current, therefore the speed of the motor can be tracked by the voltage variation according to speed change. During the conditions of the load variation, the extra power needed is achieved by the current variations with the maximal current limiter for the motor protection.

4.4.1 Conventional Controllers for bidirectional DC DC converters Using General Purpose Switch

A Bidirectional DC/DC converter implemented by the antiparallel connection of a simple non-isolated buck or boost converter consisting of a bidirectional switch is sufficient since the isolation between the two buses is not required in the automobiles and also the voltage conversion ratio of input and output is quite small i.e. about 1/3 or 3.

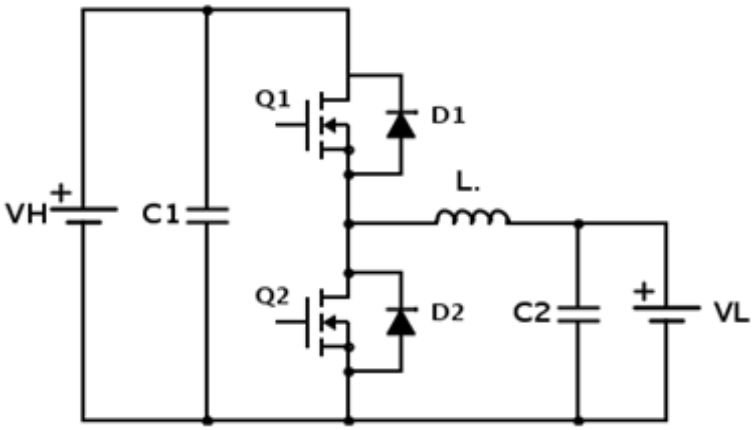

Figure 4.4: shows the bidirectional converter where switches QI and Q2 turn on and off alternatively through the main switch or the freewheeling diode according to its operating direction

Fig. 2 shows the synchronous buck/boost converter where switches Q1 and Q2 turn on and off alternatively through the main switch or the free wheeling diode according to its operating direction. This DC/DC converter is considered to be dual battery system (V1/V2), and it is connected to batteries as the loads on

both sides of the input and output. This batteries act as the voltage sources. Fig 3 is the typical controller block diagram for the above bi-directional DC/DC converter. Conventionally, for switch mode power supplies the controller of the DC/DC converter is implemented with general purpose PWM ICs. But this PWM ICs are unable to change the operating mode of the two switches without being turning off since they are being fed by a single power source. Therefore, the bidirectional converter circuit implementation with single PWM IC is quite difficult [26] . Moreover as in the case of the current mode controller employed for the bidirectional conveter, the time of the switching off for a particular switch for the mode transition is determined by comparing the switch current with the error amplifier output and therefore two PWM ICs should be used, since a particular mode can detect the variation of current in one direction only. Therefore in conventional practice two separate controllers for each mode is used and the gate drive signal from both the controllers are combined to actually turn on or off the switch. Therefore only one PWM controller remains in operation at a particular time. When the transition from one mode to the other mode is required, the particular controller that is operating has to be turned off before the turning on of the other controller.

Unified Controller Concept

A simplified approach to implement the controller is to merge both the controllers into a single unified controller with a mode switching logic according to the power flow demand [26] . Fig. 3 (a) shows that traditional way of two separate controllers: buck and boost controllers. The switch between the two different modes is controlled and operated by a power management command.The two seperate controllers can be integrated and merged into a single controller by using the complementary switching technique as shown in Fig. 3(b). Different current flow directions represent different modes.

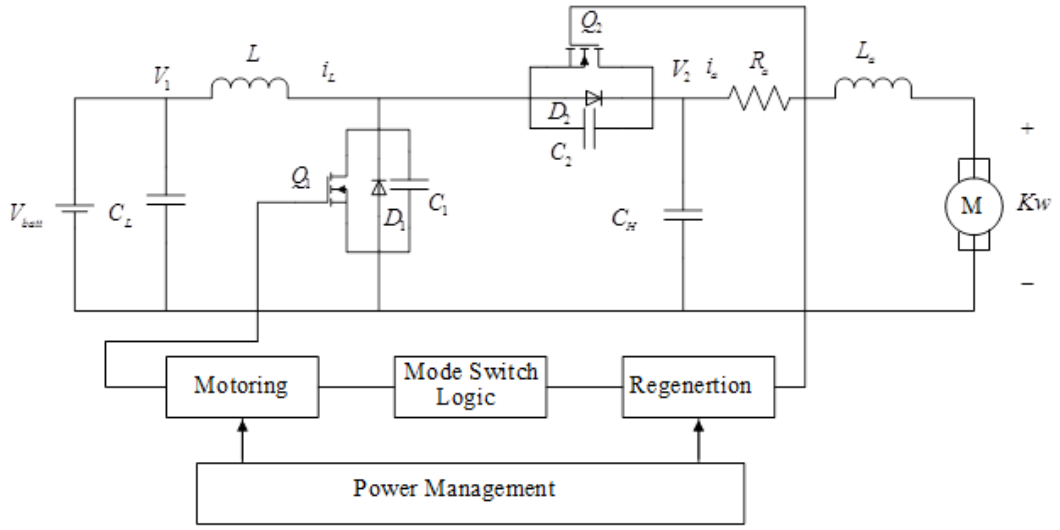

Figure 4.5: Power Stage Controlled by the Separate Controller

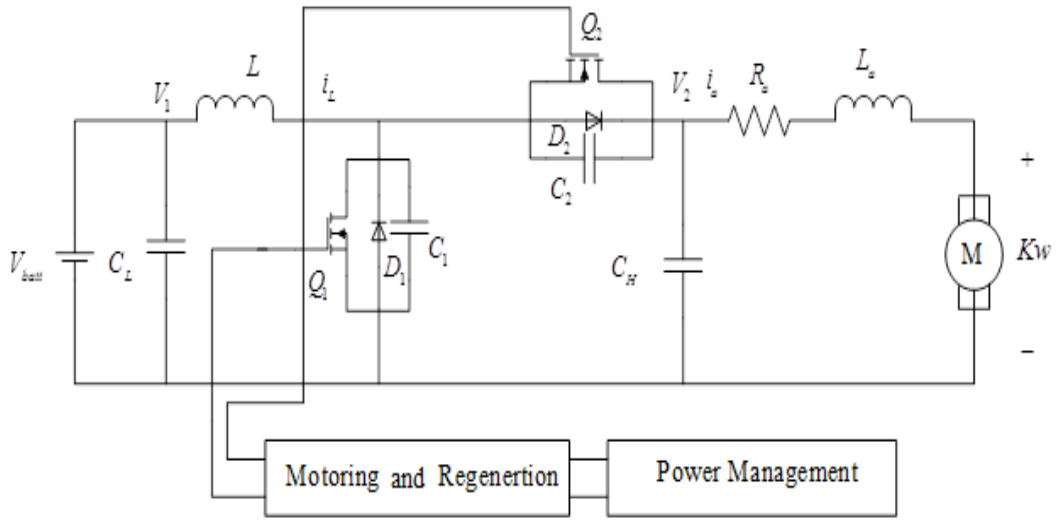

Figure 4.6: Power Stage Controlled by a Unified Controller

The present design requires the speed control of the dc motor while motoring while speed control and battery voltage regulation during regeneration. The bidirectional DC DC converter automatically shifts into buck mode or boost mode depending up on the armature current and the only thing we have to do is the speed control. Voltage control is automatically achieved by the the speed control since the motors speed is determined by the converters output voltage.

The voltage conversion ratio of the converter can be expressed as:

$$\frac{V_2}{V_{batt}} = \frac{1}{1 - D_{Q1}}$$
$$\text{and} \quad \frac{V_{batt}}{V_2} = D_{Q2}$$

where $D_{Q1} = 1 - D_{Q2}$

$$\text{and} \quad \frac{V_{batt}}{V_2} = \frac{T_{Q2_{ON}}}{T_{Q2_{ON}} + T_{Q2_{OFF}}} = D_{Q2}$$

where $T_{Q2_{ON}} = T_{Q1_{OFF}}$and $T_{Q2_{OFF}} = T_{Q1_{ON}}$

Therefore if the battery voltage is 15V and the motors armature voltage is 25V, then the nominal duty cycle required during the boost operation is equal to 2/5 or 0.4. Also, therefore the duty cycle required for the buck operation from 25V to 15V is 3/5 or 0.6 . We can draw the voltage conversion ratio $\frac{V_2}{V_{batt}}$ and the $\frac{V_{batt}}{V_2}$ versus D_{Q1} and analyse the dependency of the buck and boost operation on the duty cycle of the boost switch.

If we consider that the high voltage side bus is at 25V and the battery voltage is 15V, then from the above fig, we can observe that as long as the duty ratio of the boost switch remains below 0.4, the converter works as a buck converter and charges the battery in regeneration mode. If the duty ratio of the boost switch rises above 0.4 (i.e. for a buck switch it is below 0.6),then the converter works in the motoring mode and the battery suppies power for motor operation. Proceeding on the same analogy we can infer that for the regulation of the speed we

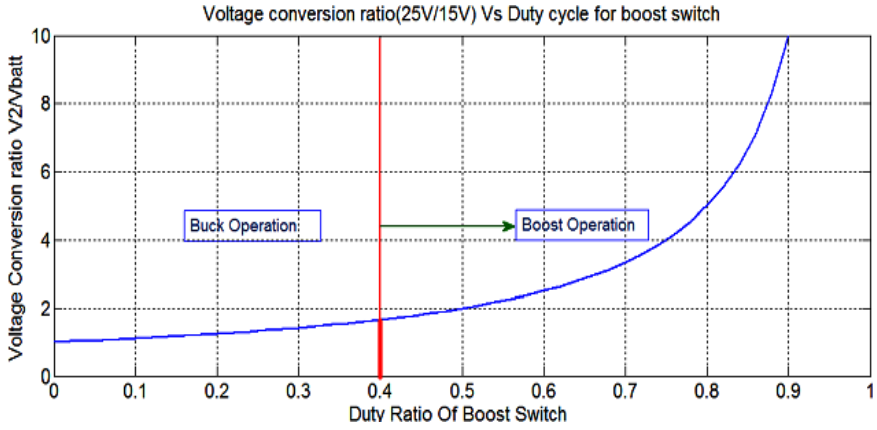

Figure 4.7: Voltage conversion ratio(15V/25V) Vs Duty cycle for buck switch

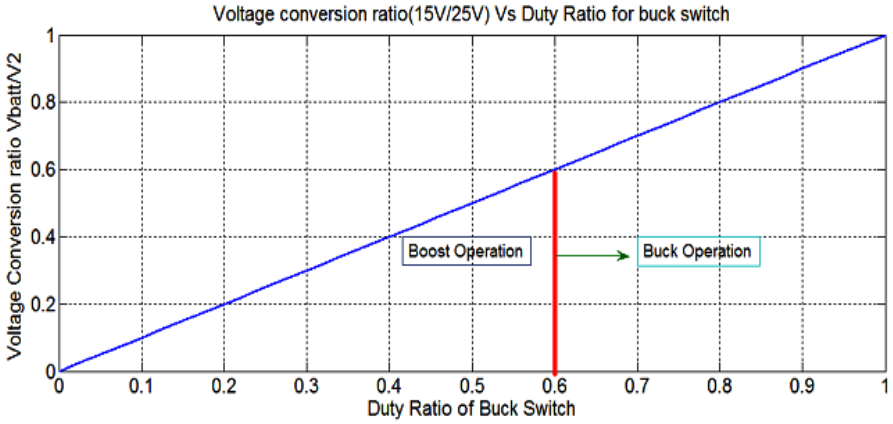

Figure 4.8: Voltage conversion ratio(25V/15V) Vs Duty cycle for boost switch

need to regulate the armature voltage for the desired speed. We can operate the converter in both the modes i.e. motoring as well as regeneration with a single PID controller for tracking speed.

Motoring Mode

In this mode of operation, the load torque and hence the motor current Ia is positive , therefore the back emf i.e K_w is always less than the motor's armature voltage by an amount equal to I_aR_a. Therefore in order to rotate the motor at the desired speed, the duty cycle adjusts itself so as to always keep the armature voltage greater than the back emf by an amount I_aR_a and hence the converter works in the boost operation at all the time while motoring.

Regeneration Mode

During downhill motion, due to the slope, a negative load torque acts on the motor. Due to the negative load torque, the motor current gets negative and hence the motor's back emf voltage rises by an amount equal to $I_a R_a$ than the armature voltage. Now if we consider that the w is the speed of the motor and we want to keep the motor rotating during at a constant speed during motoring as well as regeneration, than w is given by:
Motoring(positive load torque Tl):

$$w = \frac{V_{2m} - I_a R_a}{K}$$

During regeneration(negative load torque -Tl) :

$$w = \frac{V_{2reg} - I_a R_a}{K}$$

From the above equations we see that if we want to keep the speed constant during both the modes, than we have

$$V_{2reg} = V_{2m} - 2I_a R_a$$

Clearly, we see that the armature voltage should decrease during regeneration so as to keep the speed constant. Therefore the duty ratio of the boost switch decreases and it moves into the buck operating region and the motor acts as a generator to recharge the battery. Thus the switching between the motoring mode and the regenerative mode depends on the magnitude of the negative load torque acting on the motor, battery voltage and the speed of the motor.

PID Controller Design for the speed tracking

4.4.2 PID Controller Design for DC Motor Speed Tracking

The armature voltage across the dc motor depends on the converters output voltage which further depends on the duty cycle. Since the speed of the dc motor

is directly proportional to the armature voltage, speed can be controlled by varying duty cycle.

The speed to duty cycle transfer function as derived above is as follows:

$$\frac{\hat{w}}{\hat{d}} = \frac{-s^2 + \left(\frac{V_2(1-D)}{I_L L} - \frac{1}{R_1 C_1}\right) s + \left(\frac{V_2(1-D)}{I_L R_1 C_1 L} - \frac{1}{C_1 L}\right)}{s^5 + a_4 s^4 + a_3 s^3 + a_2 s^2 + a_1 s^1 + a_0}$$

Putting the values of the motor parameters and the steady state values of the voltages and the current in the above equation we get, the open loop bode plot of the above system is as shown below:

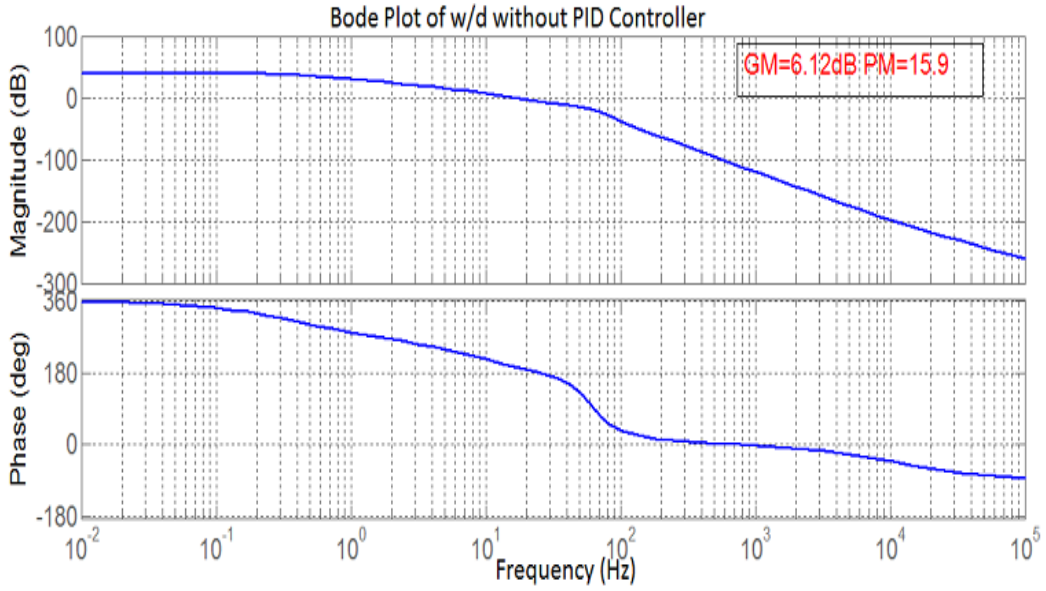

From the above Fig we see that the GM is 6.12 dB and PM is 15.9 degrees.

Also the armature voltage to duty cycle transfer function is given by:

$$\frac{\hat{v}_2}{\hat{d}} = \frac{-85.24(s - 7.04e004)(s - 47.7)(s + 2.356)}{(s + 49.94)(s + 2.238)(s^2 + 247.9s + 1.45e005)}$$

And its open loop bode plot is

Based on the step response of the w/d, a PID controller is designed on the basis of the Zeiglar Nichols, Method.

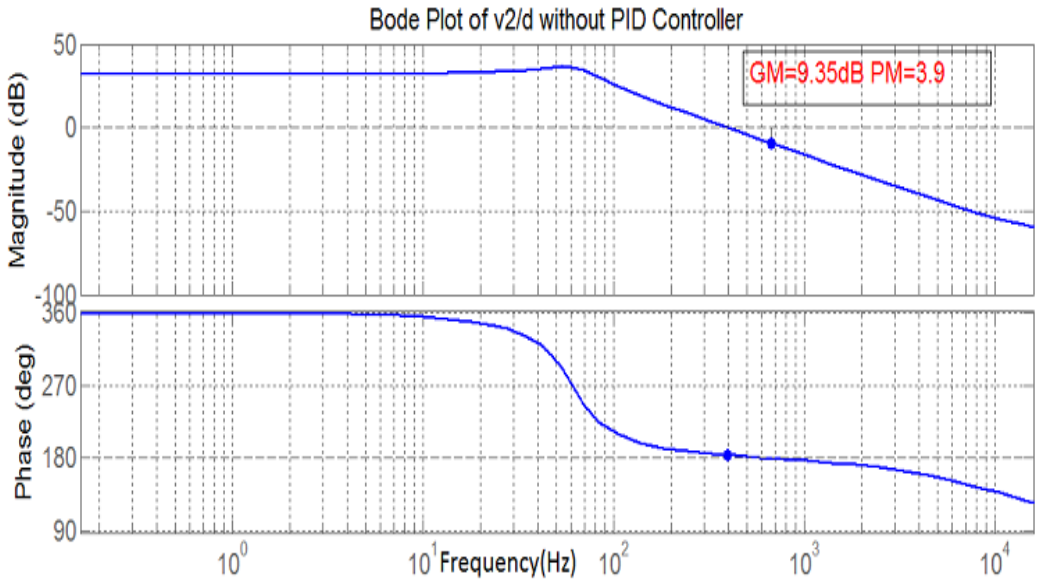

In 1942, based on time response and experiences, Ziegler-Nichols proposed a tuning formula. The main objectives of the tuning of the PID controllers are as follows:

1. To minimize the rise time Tr (Tr is the time required for system response to rise from 10% to 90% (over damped); 5% to 95%; 0% to 100% (Under damped) of the final steady state value of the desired response).

2. Minimize the peak overshoot (Peak overshoot is the maximum peak value of the response curve measured from the desired response of the system)

3. Minimize the settling time, Time required for response to reach and stay within 2% of final value.

4.4.3 PID controller

Proportional-integral-derivative (PID) controllers are widely used in industrial control systems because it has only three parameters that has to be tuned for the process control. A PID controller takes the input as an error signal which is the difference between the measured process variable and a desired reference signal. The controller minimizes the error by trying adjusting the control inputs. It involves three constant parameters that has to be tuned namely K_P the proportional

term ,K_I the integral term and K_D the differential term. Here K_P depends on the present value of the error, K_I depends on the accumulation of the errors in past where as the K_D is dependent on the rate of the change of error in the present. Its structure can be denoted as:

$$K(s) = K_P \left[1 + \frac{1}{T_I(s)} + T_D(s)\right]$$

Because of its simple structure, PID controller is the most extensive control method that is used in industry . The important characteristics of the PID controllers are :

- They can eliminate steady-state error of the step response (due the presence of the integral action)
- They can reduce the peak overshoot i.e. they can provide damping (due to derivative action)

4.4.4 Ziegler-Nichols tuning

This method is applied when the plants exhibits the step response as of the form shown in the fig below:

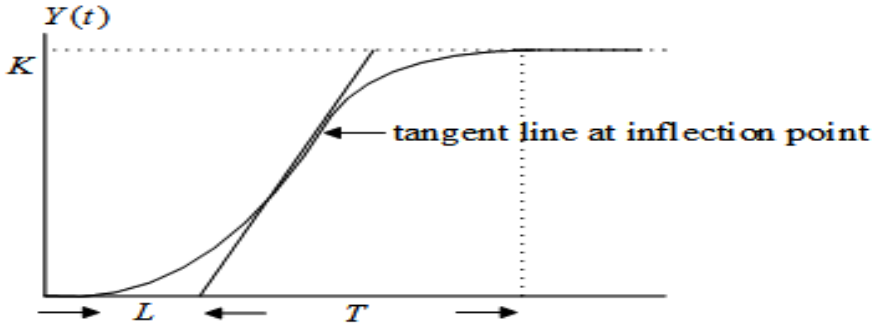

Figure 4.9: Step response curve for Zeigler Nichols parameters

This response is the characteristics of the first order system with transportation delay. The response can be characterized by the two parameters i.e the delay time

L and the time constant T. These are determined by drawing a tangent at the point of inflection of the step response and noting its intersections with the time axis and the steady state value. The plant model can therefore be given by:

$$G(s) = \frac{Ke^{-sL}}{Ts + L}$$

Based on the Ziegler and Nichols method following control parameters can be derived from this model. In real-time process control systems, a large variety of plants can be approximately modeled by the above model. If the model of the system cannot be derived mathematically, then the experiments can be done to find out the parameters of the approximate model. For eg. if the step response of the system is experimentally found out as shown in the fig then

$$K_P = 1.2T/L, \;\; T_I = 4L, \;\; T_D = .5L$$

also the parameters K_I and K_D can be found out as:

$$K_I = \frac{K_P}{T_I}, \;\; K_D = K_P \times T_I$$

Based on the above method, the step response of the w/d was obtained as follows:

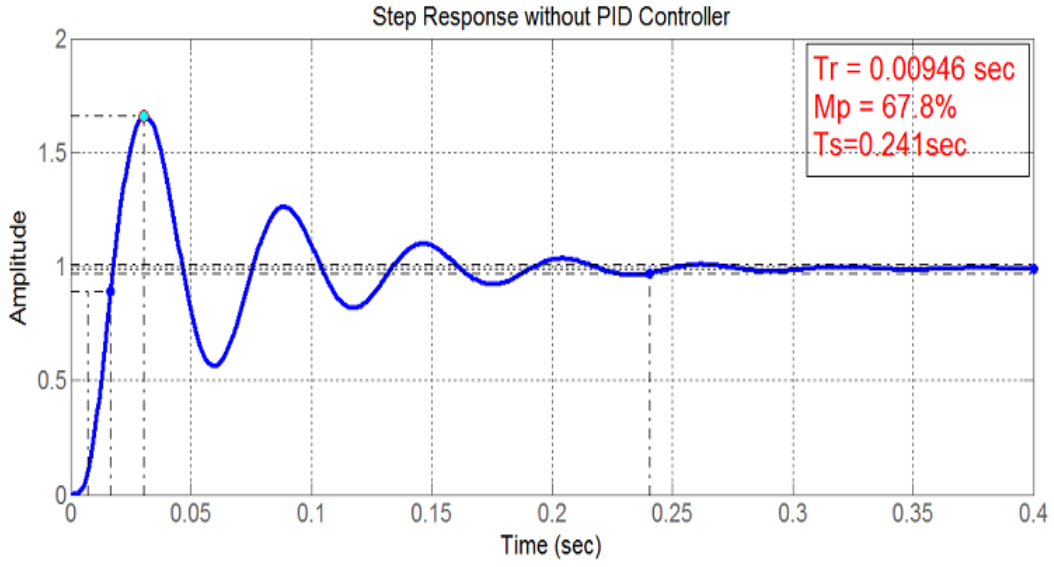

Based on the above response, the PID parameters are found as follows:

$$K_P = .1, \;\; K_I = .03 \;\text{ and }\; K_D = .0006$$

With the designed PID controller, the compensated system step response was obtained as follows:

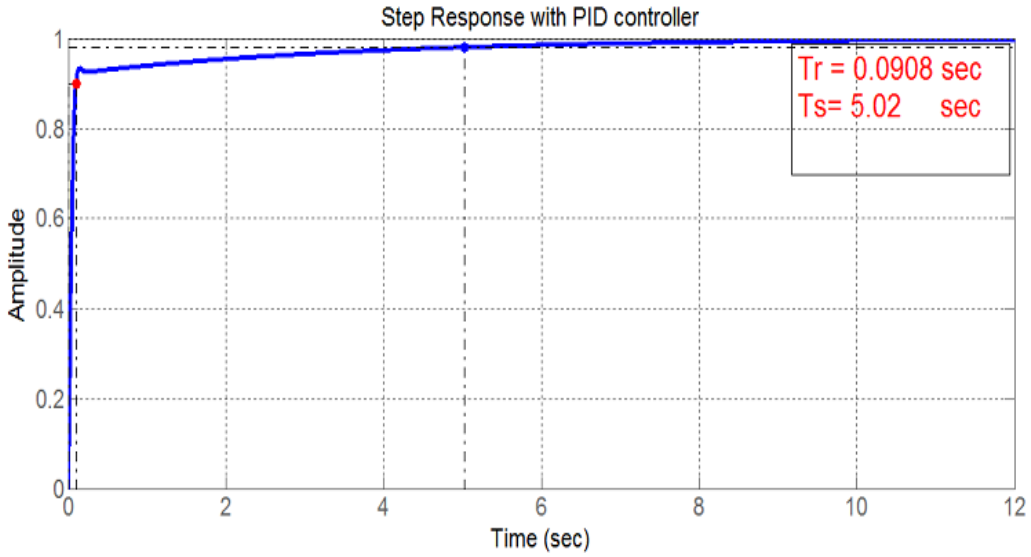

Also the bode plot of the w/d with the controller is as shown below:

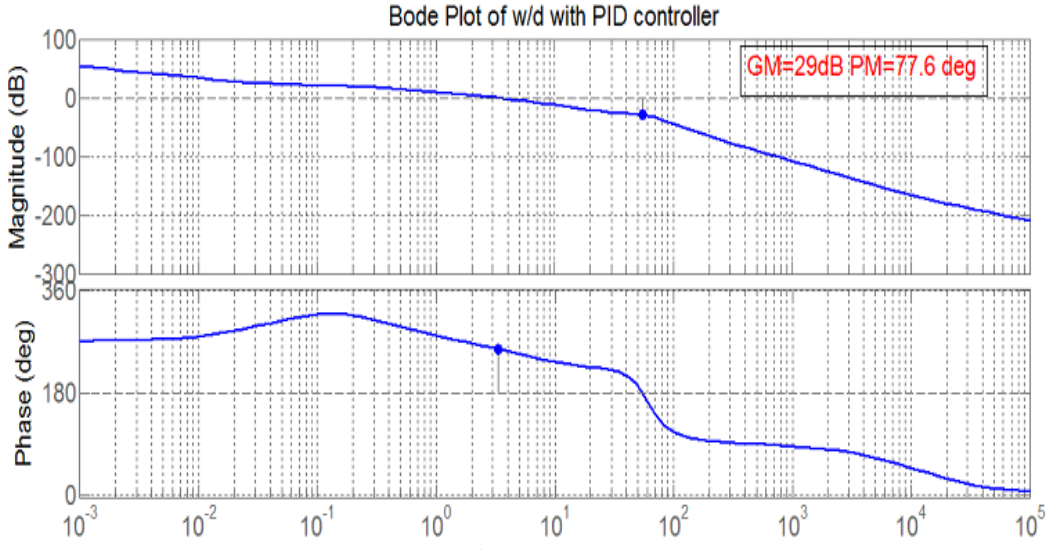

As shown in the above fig we see that the GM = 29 dB and PM=77.6 degrees for the system with PID controller.

Chapter 5

Simulation and Results

Chapter 5

Simulation and Results

Closed loop Simulation of the Bidirectional Converter fed PMDC Motor with the designed values was done in the Matlab Simulink. The simulation results were found satisfactory and as expected. The various waveforms are as follows:

1. Parasitic ringing in the DCM mode in the Bidirectional DC DC converters without complimentary Gate switching Technique.

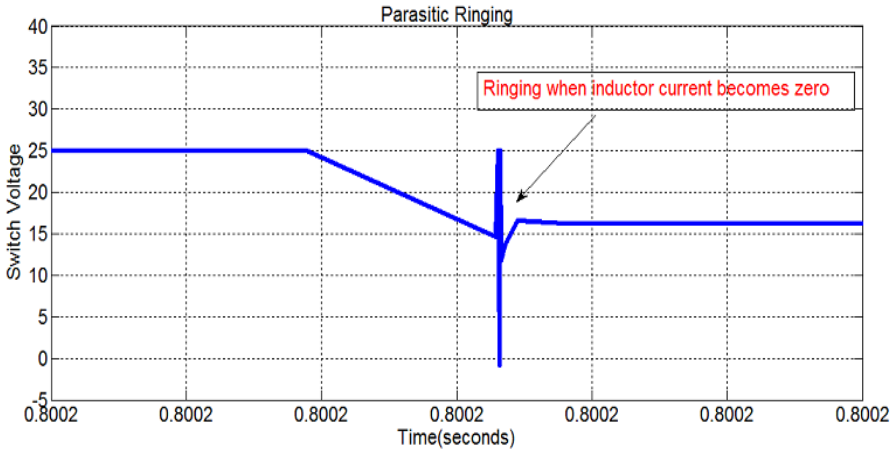

Figure 5.1: MOSFET Voltage Ringing at the zero inductor current without Soft Turn OFF switching

2. Motors Armature Voltage

   Till not 1 sec, the bidirectional converter works in motoring mode and hence the steady state voltage is near about $25V$, after 1 sec the motor is supposed to be in downhill motion. Therefore the voltage increases because the speed increases and the converter work in regeneration mode.

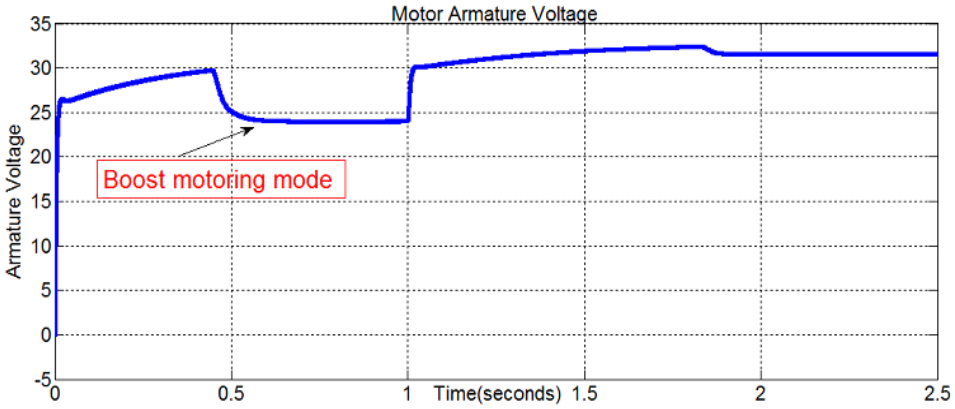

3. Motor Current

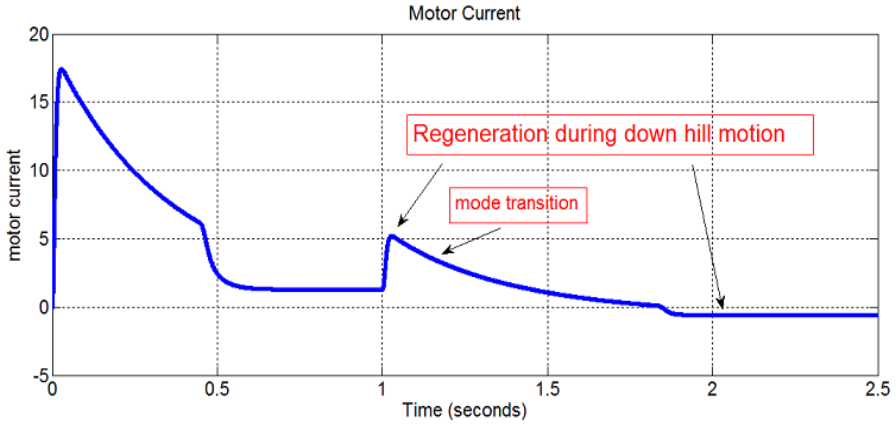

The negative current after 1 sec shows the regenerative mode; hence converter operates in the buck mode.

4. Motor torque:

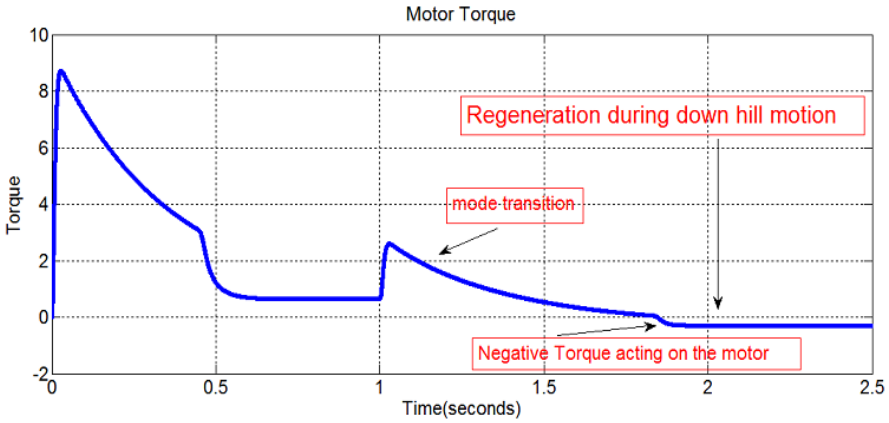

During regeneration due to downhill motion, the torque acting on the motor is negative; therefore it acts like a generator.

5. Motor Speed Tracking

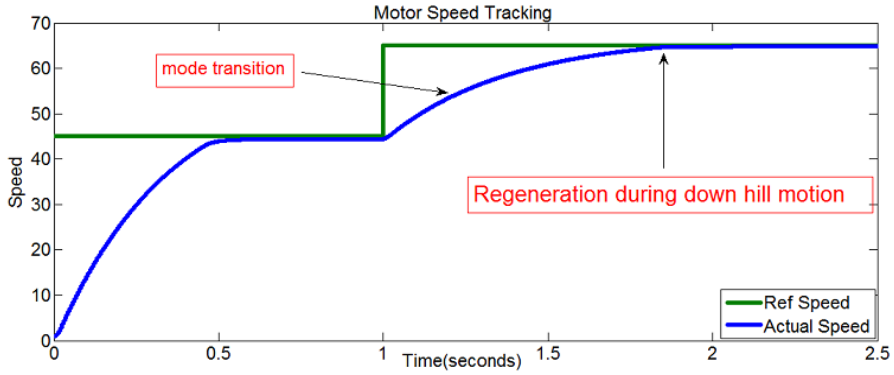

6. Battery current:

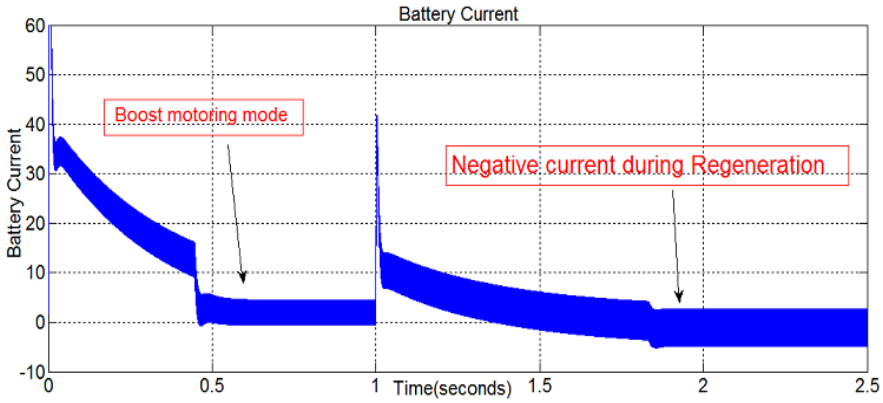

7. Battery Voltage:

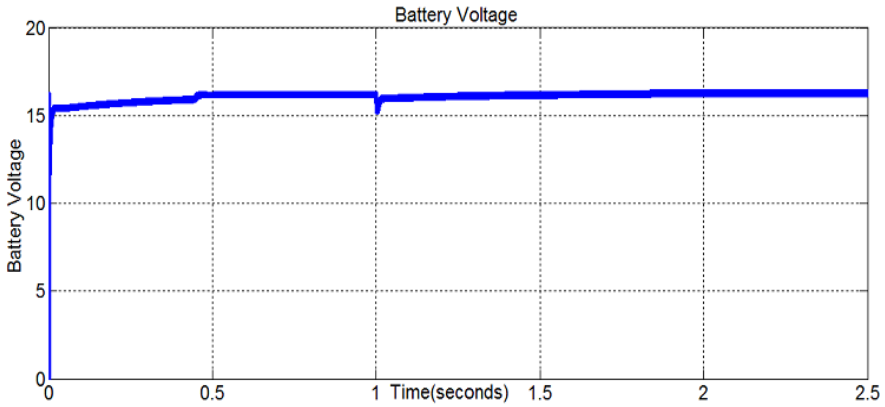

8. Battery SOC

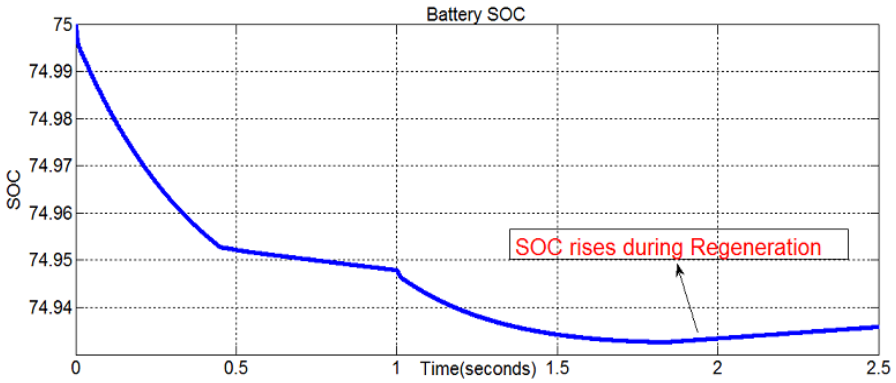

9. Boost MOSFET Current

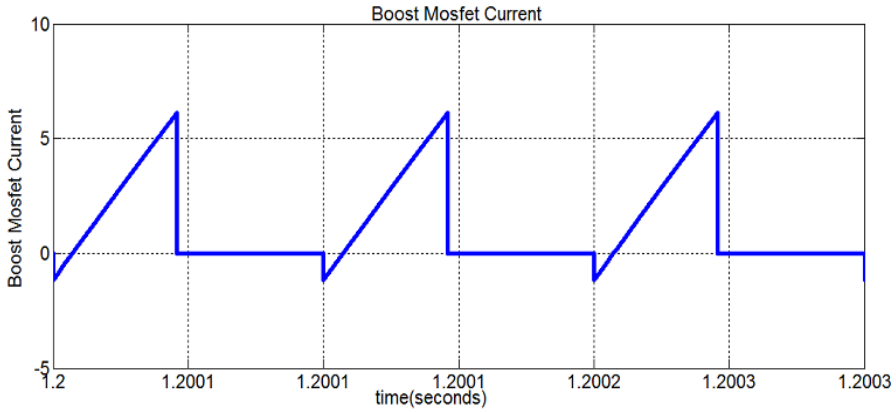

10. Boost MOSFET Voltage

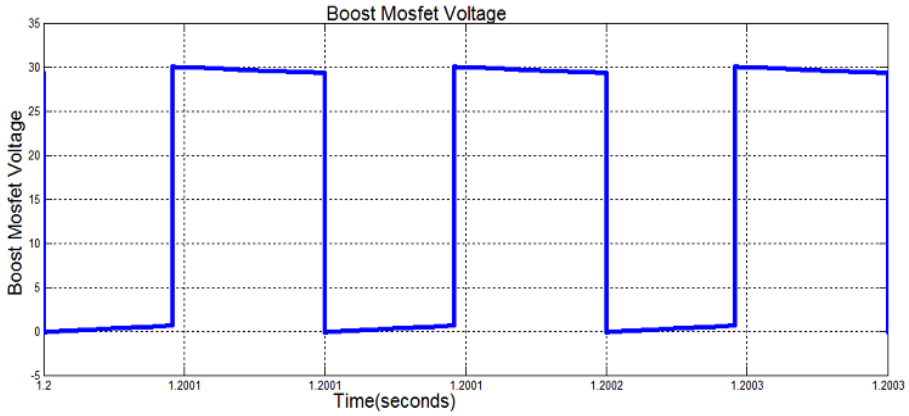

11. Buck MOSFET Current

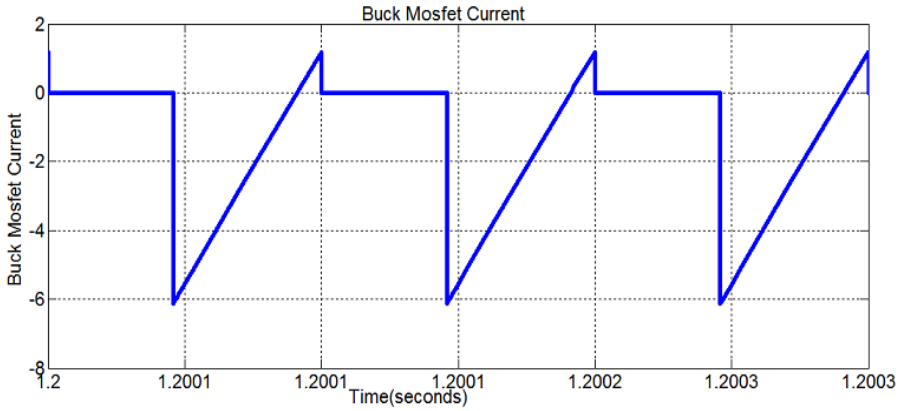

12. Buck MOSFET Voltage

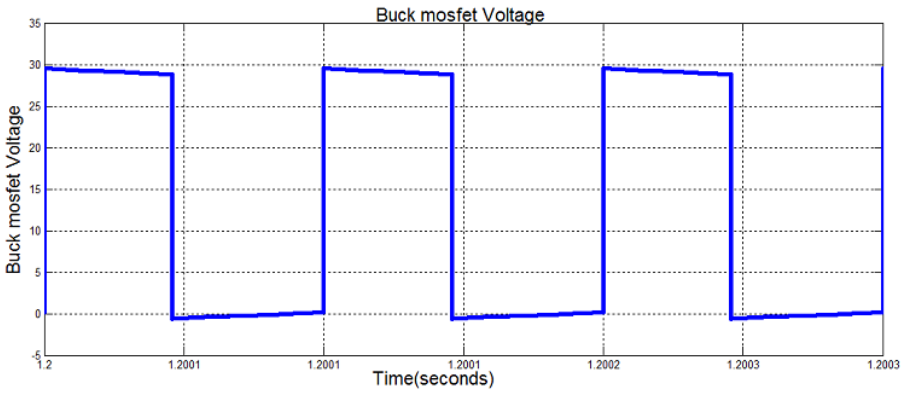

13. Switching Current

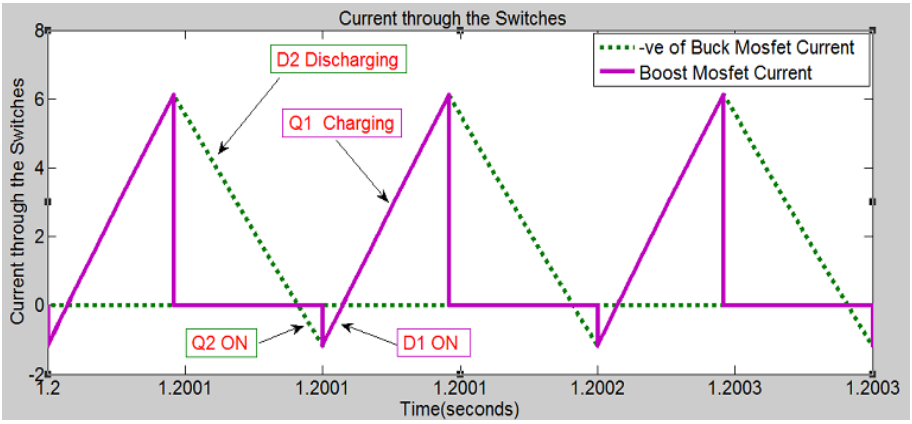

14. Inductor Current

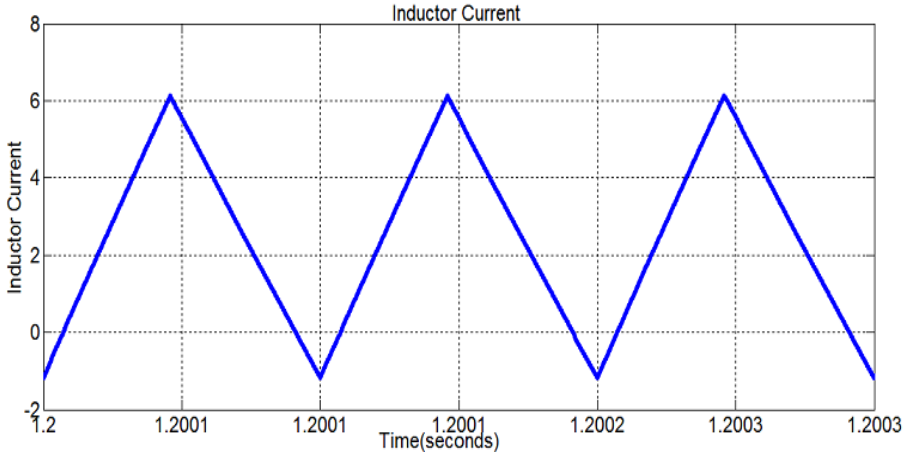

15. Regenerative Braking.

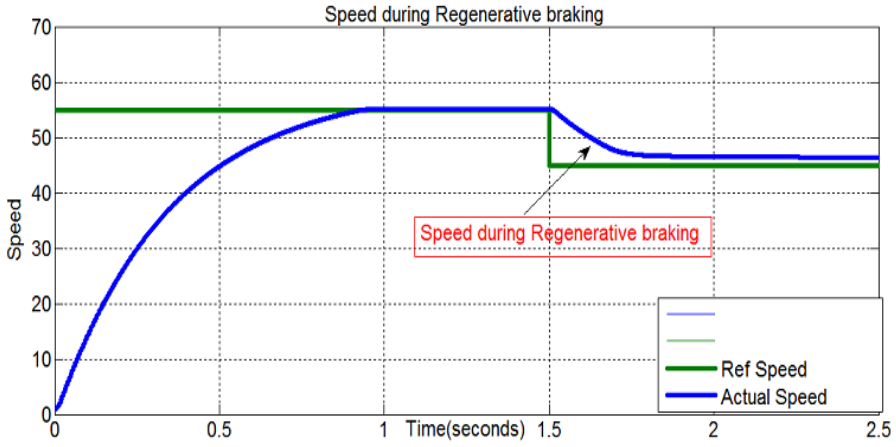

5.1 Conclusion

Speed control of the DC motor has been achieved with the designed bidirectional DC DC converter. The designed converter operating in the complimentary ZVRT switching has been simulated and the various current and voltage waveforms has been compared with the bidirectional DC DC converter without complimentary switching, which shows that the designed converter operates in the soft switching mode, and therefore the switching losses are reduced thereby increasing the efficiency.

The PID controller has been designed on the basis of the Zeigler Nichols method which considerably reduces the overshoot and has been found to work satisfactorily. Also the regenerative braking of the PMDC motor has been successfully realized thus achieving the design targets.

5.2 Future Work

With the inductor operating in the discontinuous mode, the inductor current ripple considerably rises, which can be reduced by multiphase interleaved operation. Multiphase interleaved operation will thereby also reduce the stress on the high side capacitor, thus the capacitor value can also be reduced. Presently in the design motor current control has not been implemented, which is also an important thing to realize before the hardware implementation of the above system so that the system stability can be ensured at load disturbance and can prevent the motor from damage.

Bibliography

[1] Emadi, Ali, Kaushik Rajashekara, Sheldon S. Williamson, and Srdjan M. Lukic,"Topological overview of hybrid electric and fuel cell vehicular power system architectures and configurations," *IEEE Transactions on Vehicular Technology*, 54, no. 3 (2005): 763-770.

[2] Chan, C. C., Alain Bouscayrol, and Keyu Chen,"Electric, hybrid, and fuel-cell vehicles: Architectures and modeling," *IEEE Transactions on Vehicular Technology*, 59, no. 2 (2010): 589-598.

[3] Emadi, Ali, Young Joo Lee, and Kaushik Rajashekara,"Power electronics and motor drives in electric, hybrid electric, and plug-in hybrid electric vehicles," *IEEE Transactions on Industrial Electronics*, 55, no. 6 (2008): 2237-2245.

[4] Cagatay Bayindir, Kamil, Mehmet Ali Gzkk, and Ahmet Teke,"A comprehensive overview of hybrid electric vehicle: Powertrain configurations, powertrain control techniques and electronic control units," *Energy Conversion and Management*,52, no. 2 (2011): 1305-1313.

[5] Amjadi, Zahra, and Sheldon S. Williamson,"Power-electronics-based solutions for plug-in hybrid electric vehicle energy storage and management systems," *IEEE Transactions on Industrial Electronics*,57, no. 2 (2010): 608-616.

[6] Karshenas, Hamid R., Hamid Daneshpajooh, Alireza Safaee, Praveen Jain, and Alireza Bakhshai,"Bidirectional DC-DC Converters for En-

ergy Storage Systems," *Energy Storage in the Emerging Era of Smart Grids, Rosario Carbone (Ed.)*,ISBN: 978-953.

[7] Caricchi, F., F. Crescimbini, F. Giulii Capponi, and L. Solero,"Study of bi-directional buck-boost converter topologies for application in electrical vehicle motor drives," *In Applied Power Electronics Conference and Exposition, 1998. APEC'98. Conference Proceedings 1998., Thirteenth Annual*,vol. 1, pp. 287-293. IEEE, 1998.

[8] Cao, Jian, and Ali Emadi,"A new battery/ultracapacitor hybrid energy storage system for electric, hybrid, and plug-in hybrid electric vehicles," *IEEE Transactions on Power Electronics*,27.1 (2012): 122-132.

[9] Lee, Young-Joo, Alireza Khaligh, and Ali Emadi,"Advanced integrated bidirectional AC/DC and DC/DC converter for plug-in hybrid electric vehicles," *IEEE Transactions on Vehicular Technology*,58, no. 8 (2009): 3970-3980.

[10] Liu, Wei-Shih, Jiann-Fuh Chen, Tsorng-Juu Liang, Ray-Lee Lin, and Ching-Hsiung Liu,"Analysis, design, and control of bidirectional cascoded configuration for a fuel cell hybrid power system," *IEEE Transactions on Power Electronics* 25, no. 6 (2010): 1565-1575.

[11] Shen, Z. John, and Ichiro Omura,"Power semiconductor devices for hybrid, electric, and fuel cell vehicles," *Proceedings of the IEEE 2007* 95, no. 4 (2007): 778-789.

[12] Ke, Yu-Lung, Ying-Chun Chuang, and Hung-Shiang Chuang,"Energy recovery electric bicycle with two-quadrant DC motor drivers," *In Industry Applications Society Annual Meeting, 2009. IAS 2009. IEEE* ,pp. 1-7. IEEE, 2009.

[13] Schupbach, Roberto M., and Juan C. Balda,"Comparing DC-DC converters for power management in hybrid electric vehicles," *In Electric Machines and Drives Conference, 2003. IEMDC'03. IEEE International* , vol. 3, pp. 1369-1374. IEEE, 2003.

[14] Han, Sangtaek, and Deepak Divan,"Bi-directional DC/DC converters for plug-in hybrid electric vehicle (PHEV) applications," *In Applied Power Electronics Conference and Exposition, 2008. APEC 2008. Twenty-Third Annual IEEE* ,pp. 784-789. IEEE, 2008.

[15] Zeraoulia, Mounir, Mohamed El Hachemi Benbouzid, and Demba Diallo,"Electric motor drive selection issues for HEV propulsion systems: A comparative study," *IEEE Transactions on Vehicular Technology*, 55, no. 6 (2006): 1756-1764.

[16] Xue, X. D., K. Cheng, and N. C. Cheung,"Selection of electric motor drives for electric vehicles," *In Power Engineering Conference, 2008. AUPEC'08. Australasian Universities*, pp. 1-6. IEEE, 2008.

[17] Williamson, S., M. Lukic, and Ali Emadi,"Comprehensive drive train efficiency analysis of hybrid electric and fuel cell vehicles based on motor-controller efficiency modeling," *IEEE Transactions on Power Electronics* , 21, no. 3 (2006): 730-740.

[18] Sripakagorn, Angkee, and Nartnarong Limwuthigraijirat,"Experimental assessment of fuel cell/supercapacitor hybrid system for scooters," *International journal of hydrogen energy* 34, no. 15 (2009): 6036-6044.

[19] Zhang, Junhong. Bidirectional DC-DC Power Converter Design Optimization,"Modeling and Control. Diss. Virginia Polytechnic Institute and State University,"2008.

[20] Xu, Haiping, Xuhui Wen, Ermin Qiao, Xin Guo, and Li Kong,"High power interleaved boost converter in fuel cell hybrid electric vehicle," *IEEE International Conference on Electric Machines and Drives*, 2005 , pp. 1814-1819. IEEE, 2005.

[21] Huang, Xudong, Xiaoyan Wang, Troy Nergaard, Jih-Sheng Lai, Xingyi Xu, and Lizhi Zhu,"Parasitic ringing and design issues of digitally controlled high power interleaved boost converters," *IEEE Transactions on Power Electronics*, 19, no. 5 (2004): 1341-1352.

[22] Zhang, Junhong, Jih-Sheng Lai, Rae-Young Kim, and Wensong Yu,"High-power density design of a soft-switching high-power bidirectional dcdc converter," *IEEE Transactions on Power Electronics*, 22, no. 4 (2007): 1145-1153.

[23] Hua, Guichao, and Fred C. Lee,"Soft-switching techniques in PWM converters," *IEEE Transactions on Industrial Electronics*, 42, no. 6 (1995): 595-603.

[24] Canales, Francisco, Peter Barbosa, and Fred C. Lee,"A zero-voltage and zero-current switching three-level DC/DC converter," *IEEE Transactions on Power Electronics*, 17, no. 6 (2002): 898-904.

[25] Liu, K-H., and Fred CY Lee,"Zero-voltage switching technique in DC/DC converters," *IEEE Transactions on Power Electronics*, 5, no. 3 (1990): 293-304.

[26] Yoo, Chang-Gyu, Woo-Cheol Lee, KyuChan Lee, and Inyoung Suh,"Current mode PWM controller for a 42V/14V bidirectional DC/DC converter," *In Power Electronics Specialists Conference, 2006. PESC'06. 37th IEEE*, pp. 1-6. IEEE, 2006.

[27] Yoo, ChangGyu, Woo-Cheol Lee, Kyu-Chan Lee, and Bo H. Cho,"Transient current suppression scheme for bi-directional DC-DC converters in 42 V automotive power systems," *In Applied Power Electronics Conference and Exposition, 2005. APEC 2005. Twentieth Annual IEEE*, vol. 3, pp. 1600-1604. IEEE, 2005.

[28] Huang, Xudong, Troy Nergaard, Jih-Sheng Lai, Xingyi Xu, and Lizhi Zhu,"A DSP based controller for high-power interleaved boost converters," *In Applied Power Electronics Conference and Exposition, 2003. APEC'03. Eighteenth Annual IEEE*, vol. 1, pp. 327-333. 2003.

[29] Hwang, Sentai, and J. Chou,"Comparison on fuzzy logic and PID controls for a DC motor position controller," *In Industry Applications Society Annual Meeting, 1994., Conference Record of the 1994 IEEE, pp. 1930-1935. IEEE, 1994.*